



TÉCNICO
LISBOA

**OPTIMAL DESIGN OF A STIFFENED PLATE SUBJECTED TO
COMBINED LONGITUDINAL COMPRESSION AND LATERAL
LOADS**

Yincai Huang

Thesis to obtain the Master of Science Degree in

Naval Architecture and Ocean Engineering

Supervisor: Prof. Yordan Garbatov

Jury

Chairman: Prof. Carlos Guedes Soares
Supervisor: Prof. Yordan Garbatov
Member: Prof. Angelo Teixeira

December 2018

Acknowledgements

I want to express my gratitude to all those who helped me during the writing of this thesis.

My deepest gratitude goes first and foremost to Professor Yordan Garbatov, my tutor, for his constant encouragement and guidance. Without his consistent and illuminating instruction, this thesis could not have reached its present form.

Second, I would like to express my heartfelt gratitude to Professor Carlos Guedes Soares, who helped me a lot during the master study. I am also much indebted to the professors at the Department of Naval Architecture and Ocean Engineering, who have instructed and helped me a lot.

Then, I also owe my sincere gratitude to my friends and my classmates who gave me their help and time in listening to me and helping me work out my problems during the challenging course of the thesis. Besides, I am incredibly grateful for my roommates for their cooperation, comments, and wise advice for my study and life.

Last, my thanks would go to my beloved family for their thoughtful considerations in me all through these years.

Abstract

The objective of this thesis is to design and optimise a stiffened plate, which is a part of a ship hull structure. The work performs a multi-objective structural optimisation of a stiffened plate subjected to a combined stochastic buckling and fatigue loads in minimising the structural section area, maximum displacement and fatigue damage by satisfying a predefined target reliability level. The Pareto frontier solutions calculated by the Non-Dominated Sorting Genetic Algorithm (NSGA-II) is used to define the feasible surface of the design variables. The first order reliability method is employed to identify the topology of the stiffened plate as a part of the Pareto frontier solutions in reducing the failure probability due to fatigue and buckling.

In the present study, a review of the relevant developments has been briefly discussed in the first chapter. Some fundamental theories and formulae required in the analysis are given in Chapter 2. The ultimate strength of a bulk carrier has been performed in Chapter 3. The optimisation is made by the Non-Dominated Sorting Genetic Algorithm (NSGA-II), and the reliability-based optimisation of a stiffened plate as a part of a bulk carrier has been performed and discussed in Chapter 4. Finally, some conclusions and future work are given in Chapter 5.

Resumo

O objetivo desta tese é projetar e otimizar uma placa endurecida, que é parte de uma estrutura de casco de navio. O trabalho realiza uma otimização estrutural multiobjetiva de uma placa endurecida sujeita a uma carga estriada e de fadiga combinada, minimizando a área da seção estrutural, o deslocamento máximo e o dano por fadiga, satisfazendo um nível de confiabilidade-alvo predefinido. As soluções de fronteira de Pareto calculadas pelo Algoritmo Genético de Ordenação Não Dominada (NSGA-II) são usadas para definir a superfície viável das variáveis de projeto. O método de confiabilidade de primeira ordem é empregado para identificar a topologia da placa endurecida como parte das soluções de fronteira de Pareto na redução da probabilidade de falha devido à fadiga e flambagem.

No presente estudo, uma revisão dos desenvolvimentos relevantes foi brevemente discutida no primeiro capítulo. Algumas teorias e fórmulas fundamentais requeridas na análise são apresentadas no Capítulo 2. A resistência final de um graneleiro foi realizada no Capítulo 3. A otimização é feita pelo Algoritmo Genético de Ordenação Não Dominada (NSGA-II) e a confiabilidade e a otimização baseada em uma placa endurecida como parte de um graneleiro foi realizada e discutida no Capítulo 4. Finalmente, algumas conclusões e trabalhos futuros são apresentados no Capítulo 5.

Contents

Acknowledgements.....	3
Abstract	4
Resumo	5
Chapter 1 Introduction.....	8
1.1 Fatigue of ship structures.....	8
1.2 Buckling and ultimate strength	9
1.3 Multi-objective optimisation	11
1.4 Objectives.....	15
1.5 Research works	16
Chapter 2 Multi-objective optimisation of stiffened plate	19
2.1 Stiffened plate subjected to complex loading	19
2.2 Cumulative damage assessment.....	21
2.3 Multi-objective optimisation	23
2.4 Reliability assessment	25
2.5 Summary	29
Chapter 3 Ultimate strength of bulk carrier.....	30
3.1 Basic parameters.....	30
3.2 Ultimate strength approach	31
3.3 Ultimate strength assessment	35
3.4 Summary	37
Chapter 4 Optimization of bottom stiffened plate	38
4.1 Basic parameters of selected stiffened plate	38
4.2 Loads on stiffened plate	40
4.3 Optimization based on weight and fatigue.....	43
4.3.2 Objective Function	45
4.4 Reliability-based design optimisation	46
4.5 Analysis	52
4.6 Summary	57
Chapter 5 Conclusions and future works	58
5.1 Conclusions	58
5.2 Future works	58
References.....	59

List of Figures

Figure 1 Typical bi-criterion space	25
Figure 2 Flowchart of NSGA-II	25
Figure 3 Flowchart of reliability calculation	29
Figure 4 Cross section of the Capesize bulk carrier	31
Figure 5 The Bending moment-curvature.....	32
Figure 6 Flowchart procedure for assessment of M-k	34
Figure 7 Geometric properties of sectional area	35
Figure 8 Calculated hull girder loads.....	36
Figure 9 Calculated geometric properties of sectional area	36
Figure 10 Calculated section module and rule required values	37
Figure 11 Calculated ultimate strength of hull girder	37
Figure 12 Longitudinal in bulk carrier	38
Figure 13 T-type stiffened plate cross section diagram	39
Figure 14 Local static and dynamic pressure loads.....	40
Figure 15 Pareto frontier solution- net section area vs fatigue damage	53
Figure 16 Pareto frontier solution the net section area vs displacement	54
Figure 17 Beta index as a function of the net sectional area	56

List of Tables

Table 1 Research tasks	18
Table 1 Fraction of time in different conditions.....	22
Table 2 K factor of typical stiffener support,(37)	23
Table 3 Dimensions of the longitudinal stiffeners of the bulk carrier	30
Table 4 Material properties of the bulk carrier.....	31
Table 5 Original geometric parameters of stiffened plate	39
Table 6 Distribution factor F_M	40
Table 7 Two loading conditions and fraction of time.....	46
Table 8 The still water and wave-induced bending moments	46
Table 9 The Weibull shape factor and the reference period and wave	46
Table 10 Statistical parameters of ultimate bending moments.....	49
Table 11 Wave-induced vertical bending moment statistical descriptors	50
Table 12 Wave-induced dynamic pressure statistical descriptors	50
Table 13 Coefficients for calculating the mean and standard deviation of still water bending moment	51
Table 14 Mean and standard deviation of still water bending moment	51
Table 15 Statistical descriptors of still water bending moment.....	51
Table 16 Statistical descriptors of X	52
Table 17 Design solutions of Pareto frontier.....	Error! Bookmark not defined.
Table 18 Beta index under different condition and the final reliability index.....	Error! Bookmark not defined.

Table 19 Beta index vs. corresponding objective function values	55
---	----

Chapter 1 Introduction

1.1 Fatigue of ship structures

As early as 1962, Vedeler [1] noticed that ship designers in Norway and Sweden thought that for ordinary ships, the problem of fatigue was more important than the issue of the brittle fracture. He also noticed that fatigue cracks often occur in the forepeak area, at the bottom of the ship in the midship section area, at the port wall at both ends of the bridge and the corner of the big opening. However, this has not attracted worldwide attention. The real emphasis on fatigue failure of ship structures began in the late 70s. At that time, Jordan and Cochran [2-3] took several years to carefully investigate the nodes of the 86 ships of 7 ship types that were in service and found many fatigue cracks. Their work confirms the importance of fatigue damage in ship damage. Munse et al. [4-5] discussed the fatigue strength method and based on this have provided the corresponding S-N curves for the 634 typical welded joints as defined by Jordan and Cochran. Fatigue cracks often occur in large opening corners of container ships. Chen et al.[6] proposed a method to predict fatigue life by measuring the strain at the edge of a big opening. Clarke [7-8] studied the fatigue damage in the British surface ships and found that a typical military vessel had a hundred fatigue cracks in her service life, the length of the most extended crack size reached about 0.5m. Given the uncertainty of the fatigue strength assessment process, Wirsching and Chen[9] proposed that the method based on the probabilistic theory should be used, that is, the reliability analysis of fatigue life. However, until then, the research on fatigue strength was mainly concentrated in universities or some research institutions and had not attracted any particular attention from the classification societies.

In 1990, the US Coast Guard (USCG) announced that they collected 69 damaged tanker data from 1984 to 1988, except for collisions and aground, stopping at the

Valdez and Alaska where fatigue and fracture caused more than 80% of the structural damage. The Lloyd's register reported that between 1980 and 1994, 70 of more than 20 thousand tons of bulk carriers were missing due to structural damage. What is particularly notable is that there are 12 in 1990 and 13 in 1991. These events lead to a careful review of their design rules, especially in the sense that the fatigue strength check must be involved in the design rules, that is, whether the fatigue strength of the ship's node should be seriously considered at the ship design stage. This decision further promotes the development of fatigue strength research [10-12]. The International Conference on ship structural mechanics held every three years provides a lot of research literature on this subject [13-15]. The marine structure Committee of the United States has conducted an internal seminar to discuss how to prevent fatigue and fracture of ship structures [16].

The earliest formal method of the fatigue strength assessment was included in the code of ship design by GL [17]. Then the other major classification societies, such as DNV [18], ABS [19], BV [20], KR [21], LR [22], NK [23], RINA [24] and others also established their fatigue strength checking method respectively. However, through the preliminary comparison and research, it is found that there are significant differences between the methods provided by different classification societies. So the most significant problem at that time is not to make the theoretical methods better, but to unify these methods which may establish standards of different classification societies with certain comparability. In 2006, the International Association of Classification Society (IACS) published the *Common Structural Rules for Bulk Carrier* (CSR BC) and the *Common Structural Rules for Oil Tanker* (CSR OT), for the first time in the history of carrying out a unified ship structure specification on the global scale, which had a profound impact on the shipbuilding industry.

1.2 Buckling and ultimate strength

When the load reaches a particular value, and if a small increment is added, the equilibrium position of the structure will significantly change. This case is called

structural instability or buckling, and the corresponding load is called the buckling load.

The buckling problem of structures can be divided into elastic, plastic and elastoplastic buckling according to the material properties and working stress levels of structural buckling [25]. Elastic buckling occurs when the structure is still in an elastic state under the assumption of small deflection before and after buckling. Plastic buckling occurs when the structure is buckling under plastic stress, it is called plastic buckling. Elastoplastic buckling is a form of buckling, which is between elastic and plastic buckling. The pre-buckling structure is in the state of elastic behaviour then a part of the material enters the plastic state due to the disturbance and deformation, that is, the material is in the elastoplastic stress-state after the buckling. Because the material properties of these three buckling phenomena are substantially different, the whole buckling process also shows some unique features respectively. Usually, the elastic and plastic buckling are mostly studied, and the elastoplastic buckling remains a field that demands further attention. The main reason is that the theoretical analysis becomes a complicated process because of the change in the properties of the material at the junction of elastic and plastic state.

In general, there are two ways to calculate the buckling and ultimate strength of hull plates:

- 1) A simplified method based on the plate theory;
- 2) Experiment and finite element calculations

The finite element method is versatile and time-consuming. Because of the simplification, the simplified method can only be applied to specific conditions with considerable limitations, though it is convenient to use.

Plate, stiffened plate and panel are widely used in ship structure. With the trend of high speed and lightweight and the extensive use of high strength materials, the problem of buckling and ultimate strength of ship structures is particularly prominent [26]. Buckling and ultimate strength are calculated to get the maximum load capacity of hull structures against external loads. They are essential for correctly grasping the safety, economy and ensuring enough strength margin of the hull structure.

The ultimate strength of the hull structure can be determined by estimating the resistance of the structure to the following four failure modes [27]:

- Buckling or post-buckling instability;
- Plastic collapse caused by buckling;
- Brittle fracture under overload;
- Fatigue fracture caused by the repeated action of stress pulsation.

Stiffened panels are the main components of the hull structure, such as a deck, bottom, bulkhead, broadside and so on. When the external load reaches a specific value, the ultimate failure of the hull will be caused by the inability of the stiffened panel. Therefore, it is of a great engineering significance to study the buckling and ultimate strength of hull plates concerning the ultimate strength of ship hulls [28].

The ship structure is subjected to a variety of external loads, including cargo pressure, water pressure, wave-induced load and the ship hull is subjected to shear stress, bending moment, torque and so on. As a part of a ship structure, loading on a plate and stiffened plate structures can be divided into two types:

- 1) In-plane load, including an axial load (compressive stress and tensile stress), edge shear stress and in-plane axial bending stress;
- 2) Lateral load, usually caused by water pressure and cargo pressure.

The buckling deformation of the hull stiffened plate depends on many factors including the geometric size, material properties, load characteristics, initial defects (such as initial and residual stresses), boundary conditions, corrosion, fatigue cracks and so on.

1.3 Multi-objective optimisation

With the development of human society, many decision-making problems in the real world tend to be more complicated. The mathematical models constructed by a single objective are often insufficient to describe all characteristics of the problem. The mathematical models of practical issues often contain multiple solutions, that is,

multi-objective optimisation decision is needed.

In the problem solving of the multi-objective optimisation, because each target is conflicting with each other, the so-called optimal solution to make all sub-objectives optimal at the same time does not exist. The optimality of a goal often decreases the optimal degree of other goals.

The solution of a multi-objective problem is not one solution, but a set of solutions. Vilfredo Pareto named the solution set as a Pareto Optimal Solution in 1896 [29]. It is the key to solve the multi-objective problem that how to get the solution set which is sufficiently close to the ideal solution set, evenly distributed and wide in the scope.

The treatment of constraint conditions is the key to solve constrained multi-objective optimisation problems. The usual methods include a rejection of the infeasible solutions, penalty function method and a variety of correction algorithms. It is challenging to reject the feasible solution in the iterative process from the beginning to the end, especially when the feasible domain is very tiny. Repeat testing will affect the speed of solving. Various correction algorithms are designed for specific problems which are lack of universal property. The penalty function method is the most classical method to deal with constraints at the present because it is simple, but the penalty factor has the problem relevance and is not easy for the user to grasp.

In recent years, the method of transforming the constraints into optimisation objectives has been concerned.

1.3.1 Classical multi-objective optimisation algorithm

The strategy adopted by the classical methods to solve multi-objective optimisation problems is to transform the multi-objective problems into a single objective problem. According to the difference of the problems, we first assign a weight value to each objective, then add each sub-objective together to convert it into a single objective function to solve the problem. The critical point is the calculation of the weight value. Conventional methods are the weighted, constraint and goal

programming methods.

When solving multi-objective problems, traditional methods need to have specific prior knowledge of the particular problems and have significant limitations on the shape of the problem functions. As the operation mechanism of the single objective solution is adopted, only one Pareto optimal solution can be obtained in each run, and it often needs to run many times to get the optimal set of the Pareto frontier. Besides, each time the process is independent, there is no correlation between each other, the decision-makers should choose according to the specific problems, so it often needs much time to optimise by getting enough number of the Pareto solutions.

1.3.2 Development of multi-objective evolutionary algorithm

The evolutionary algorithm simulates the evolution of the biology, uses the global search of the problem space through the particular iteration in the population and can get multiple Pareto optimal solutions in an iterative process, which is suitable for solving the multi-objective optimisation problem. In 1985, Schaffer put forward the vector-evaluated genetic algorithms (VEGA) [30] method for solving the multi-objective problem and gained recognition. After that, scholars from different countries began to study evolutionary algorithm, many evolutionary algorithms with different evolutionary mechanisms are designed.

In 1987, Gold and Richardson proposed the concept of fitness sharing in solving multimodal function. To the diversity of the solution, its premise is that the solution space distribution is homogeneous and also the user should have adequate prior knowledge and precise understanding of the problem [31]. In 1993, Fonseca and Fleming proposed the Multi-Objective Genetic Algorithm (MOGA) [32]. Two years later, Srinivas and Deb introduced the Non-Dominated Sorting Genetic Algorithm(NSGA) [33]. In the same year, Horn and Nafpliotis proposed the Niche Pareto Genetic Algorithm(NPGA) [34].

There are three deficiencies in NSGA by Srinivas and Deb[33].

1) It is very time-consuming in the construction of the optimal solution set and a high calculational complex degree, $O(rN^3)$ (r -the target number, N - the number of evolution group individual), it requires constructing the non-dominating sets in every iteration. It is vast time-consuming when the problem is involved with a big N and r .

2) The elite reservation strategy, which can not only prevent the loss of the optimised solution in the calculation but also improve the performance of the algorithm, is not adopted.

3) It is not easy to determine shared parameters. The value of the shared parameter mainly ensures the species diversity, and the determination and adjustment of the shared parameters have some subjectivity.

Based on NSGA and focused on these deficiencies, Deb and his co-workers proposed a very classic NSGA-II algorithm. NSGA-II algorithm is better than the NSGA algorithm which is reflected in the following aspects:

- 1) It adopts a fast non-dominated sorting algorithm. On the one hand, its computational complexity is reduced. On the other hand, it combines the parent population with the progeny population so that the next generation of the population is selected from the double space, thus preserving all the most outstanding individuals;
- 2) The comparison operator of crowding degree and crowding degree is adopted to replace the shared radius share Q which needs to be specified, and as the winning standard in the same level comparison after the fast sorting, the individual in the quasi Pareto domain can be extended to the whole Pareto domain and distributed evenly and the diversity of the population is maintained;
- 3) The elitist strategy is introduced to ensure that some exceptional individuals are not discarded during evolution, thus improving the accuracy of optimisation results.

Using the comparison operator of crowding degree, it not only overcomes the defects that the NSGA needs to specify the shared parameters in the population, but also makes it a comparison standard among individuals in the population, so that the individual in the quasi Pareto domain can be extended to the whole Pareto domain,

and diversity of the population is guaranteed.

1.4 Objectives

Steel stiffened plates are predominantly used in ship structural design. Stiffened panels are generally adopted in the ship and offshore structures, which are subjected to the axial load and lateral pressure. For the ship structure safety, it is vital to predicting the load carrying capacity. The external bottom plating and the lower parts of the side shell are mainly subjected to the uniaxial and biaxial compressive loads, and moreover to the relatively high external lateral pressure. The effect of the lateral pressure on the plate collapse strength depends on the interaction of the axial compression, and the lateral pressure is usually accounted for by including an additional term in the interaction Eqns used for biaxial loads [35].

A genetic algorithm with termination criteria is employed here for a non-linear optimisation problem in defining the best design solutions of the stiffened plate subjected to compressive loads and lateral pressure. The genetic algorithm accommodates the fast non-dominated sorting procedure, implementing an elitism for the multi-objective search, using an elitism preserving advanced approach allowing both continuous and discrete design variables.

The objective here is to perform a multi-objective, nonlinear structural optimisation of a stiffened plate subjected to combined stochastic compressive loads accounting for the fatigue and ultimate strength and reliability based constraints in the design. The Pareto frontier, fatigue, ultimate limit state, and target reliability, defined as additional constraints are employed to identify the optimal design solution[35-36, 38].

Ultimate limit state method has been widely used in the ship design [39]. The recent development in structural reliability methods and optimisation tools permits a coupled reliability-based design approach to be employed in which the uncertainties related to the design variables can be directly accounted for.

The FORM (first order reliability methods) approaches have been used for structural

assessment as shown in [40,41], but may also be employed for a probabilistic analysis of different practical applications [34]. The reliability analysis explored here is the FORM that provides a way of evaluating the reliability with a reasonable accuracy, which is adequate for practical applications.

The primary objective is to optimise the dimensions of a ship stiffened plate. The estimation of some primary input data such as the loads on the ship is based on the empirical formula. It is optimised in the absence of specific and detailed data from a particular ship, so the classical method is not applicable here because it is hard to give the criteria for determining whether the feasible solution is retained or not. The aim of this work is to perform a multi-objective optimisation of the stiffened plate in the ship and get a complete method flow for solving such problems that are suitable for a variety of ships at the same time. So the author has chosen the NSGA-II here to ensure that in the case of only knowing the main dimensions of the ship, one can fast get the optimal solutions with enough quality and accuracy.

1.5 Research works

The Pareto frontier is applied for simultaneous minimisation of the net sectional area, structural displacement and fatigue damage.

Employing the Pareto Frontier, an optimal solution accounting for the existing constraints may be chosen using a utility function to rank the different designs, or by using 2D or 3D scatter diagrams to identify the more attractive ones. In the present study, an additional constraint is introduced representing the target reliability level to choose the most appropriate design solution.

A three-step approach for the design of stiffened plate that couples the reliability methods and structural optimisation techniques are presented. Once the structural topology is defined, the scantling of the structural components of the stiffened plate is performed and optimized, in which the design variables, objective functions related to the minimum net section area, which leads to a minimum weight, minimum displacement, minimum fatigue damage and constraints, including the

ultimate compressive strength are defined in a purely deterministic manner. Then the Pareto frontier is used to determine the most suitable design solutions in minimising the three objective functions, satisfying all constraints. The design solutions at the Pareto frontier are used to determine the most suitable design solutions, satisfying all constraints. The results are then used as a basis for the target reliability-based optimisation which is required to guarantee structural integrity. This step accommodates the uncertainties related to the design variables and involved computational models. The task related to the present study are presented in Table 1.

Table 1 Research tasks

Define the target ship hull structures	
Estimate the still water and wave-induced loads	
Ship structural design (not part of this thesis)	
Ultimate strength assessment estimate	
Identify the bottom stiffened plate as an optimization target	
Estimate the maximum deflection and stresses of the stiffened plate subjected to axial tensile/compressive load and lateral pressure	
S-N fatigue damage assessment	
Pareto Frontier solutions based on the NSGAI multiobjective optimisation accounting for:	
the minimum weight of stiffened plate f_1 ,	
the minimum mid-span displacement f_2 ,	
the minimum fatigue damage f_3 as the objective functions	
the maximum ultimate strength	
Additional constraint arisen from the acceptable target beta reliability index range	
Optimal design solution accounting for the reliability constraints	
Analysis and discussed	

Chapter 2 Multi-objective optimisation of stiffened plate

2.1 Stiffened plate subjected to complex loading

The differential Eqn of a simply supported beam subjected to a uniformly distributed lateral load q_{local} and an axial force, T can be presented as [49,52]:

$$EIz^{IV} - Tz'' = q(x) \quad (2.1)$$

where the solution of the differential Eqn can be defined as:

$$z = z_{gs} + z_{ps} \quad (2.2)$$

The general solution of the differential Eqn concerning the displacement, z_{gs} is given by:

$$z_{gs} = A_1 + A_2 kx + A_3 ch(kx) + A_4 sh(kx) \quad (2.3)$$

And the particular solution, z_{ps} is defined as:

$$z_{ps} = -\frac{qx^2}{2T} \quad (2.4)$$

The origin of the assumed coordinate system is located at the middle of the span of the stiffened plate. Since the elastic line of the beam is symmetrical concerning the centre of the span of the stiffened plate $A_2 = A_4 = 0$ and

$$z(x) = -\frac{qx^2}{2T} + A_1 + A_3 ch(kx) \quad (2.5)$$

The coefficient A_1 and A_3 are defined taking into account the boundary conditions at the supports:

$$x = \pm \frac{l}{2} \begin{cases} z = 0 \\ z'' = 0 \end{cases} \quad (2.6)$$

resulting in a system of Eqns:

$$\begin{cases} A_1 + A_3 ch\left(\frac{kl}{2}\right) = \frac{ql^2}{8EI k^2} \\ A_3 k^2 ch\left(\frac{kl}{2}\right) = \frac{q}{EI k^2} \end{cases} \quad (2.7)$$

That defines the coefficients A_1 and A_3 as

$$A_1 = \frac{q}{EI k^4} \left[\frac{k^2 l^2}{8} - 1 \right] \quad (2.8)$$

$$A_3 = \frac{q}{EI k^4} \frac{1}{ch\left(\frac{kl}{2}\right)} \quad (2.9)$$

Substituting A_1 and A_3 in the general solution, and taking that into account

$$u = \frac{kl}{2} = \frac{l}{2} \sqrt{\frac{T}{EI}} = \frac{l}{2} \sqrt{\frac{\sigma_{global} A}{EI}} \quad (2.10)$$

in the case of a compressive axial force load, $T^* = T < 0$, the maximum displacement and bending moment at $x=0$ are defined as:

$$z_{x=0}(u^*) = -\frac{5}{384} \frac{ql^4}{EI} f_0^*(u^*) \quad (2.11)$$

$$m_{x=0}(u^*) = \frac{ql^2}{8} \phi_0^*(u^*) \quad (2.12)$$

Where the magnification functions, $f_0^*(u^*)$ and $\phi_0^*(u^*)$ with respect to the displacement, $z_{x=0}(u^*)$ and bending moment, $m_{x=0}(u^*)$, in the case $T^* < 0$, are given as:

$$f_0^*(u^*) = \frac{24}{5(u^*)^4} \left(\frac{1}{\cos(u^*)} - \frac{(u^*)^2}{2} - 1 \right) \quad (2.13)$$

$$\phi_0^*(u^*) = \frac{2}{(u^*)^2} \left(\frac{1}{\cos(u^*)} - 1 \right) \quad (2.14)$$

Where:

$$u^* = \frac{kl}{2} = \frac{l}{2} \sqrt{\frac{T^*}{EI}} \quad (2.15)$$

$$T^* = \frac{\pi^2 EI}{l^2} \quad (2.16)$$

In the case when $u^* = \pi/2$ buckling failure occurs since $f_0^*(u^*) = \phi_0^*(u^*) = \infty$.

The maximum stress in the beam is

$$\sigma_{max} = \frac{T^*}{A} - \frac{m_{x=0}}{W} \quad (2.17)$$

2.2 Cumulative damage assessment

For calculating the fatigue damage of a ship structural detail, the corresponding S-N curve should be selected, and the stress range at the hot spot should be calculated. For welded structures, the S-N curve D is recommended [39]. The long-term distribution of stress ranges at local details can be described by the Weibull distribution:

$$Q(\Delta\sigma) = \exp \left[- \left(\frac{\Delta\sigma}{q} \right)^h \right] \quad (2.18)$$

Where:

Q = probability of exceedance of the stress range $\Delta\sigma$

h = Weibull shape parameter

q = Weibull scale parameter, defined as

$$q = \frac{\Delta\sigma}{(\ln n_0)^{1/h}} \quad (2.19)$$

The stress range distribution may also be expressed as

$$\Delta\sigma = \Delta\sigma_0 \left[\frac{\ln(n)}{\ln(n_0)} \right]^{1/h} \quad (2.20)$$

Where

$\Delta\sigma_0$ = reference stress range value at the local detail exceeded once out of n_0 cycles

n_0 = total number of cycles associated with the stress range level $\Delta\sigma_0$

The Weibull shape parameter may be established from long-term wave load analysis.

The shape parameter may be taken as:

$h = h_0$ For deck longitudinals

$h = h_0 - 0.005T_{act}$ For bottom longitudinals

Where:

h_0 = basic shape parameter

$$= 2.21 - 0.54 \log_{10}(L)$$

When the long-term stress range distribution is defined by applying Weibull distributions for the different load conditions and a one-slope S-N curve is used, the

fatigue damage is given by:

$$D = \frac{v_0 T_d}{a} \sum_{n=1}^{N_{load}} p_n q_n^m \Gamma \left(1 + \frac{m}{h_n} \right) \leq \eta \quad (2.21)$$

Where:

- N_{load} = total number of load conditions considered
- p_n = fraction of design life in load condition n, $\sum p_n \leq 1$, but normally not less than 0.85
- T_d = design life of ship in seconds (20 years = $6.3 \cdot 10^8$ secs.)
- h_n = Weibull stress range shape distribution parameter for load condition n,
- q_n = Weibull stress range scale distribution parameter for load condition n
- v_0 = long-term average response zero-crossing frequency
- $\Gamma(1 + \frac{m}{h_n})$ = gamma function.

In simplified fatigue calculations, the zero-crossing-frequency may be taken as

$$v_0 = \frac{1}{4 \cdot \log_{10}(L)} \quad (2.22)$$

Where L is the ship rule length in meters.

For vessels intended for regular trading, the fraction of the design life in loaded and ballast conditions, p_n , can be taken from Table 2 below:

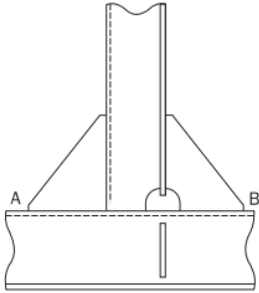
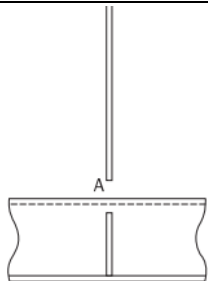
Table 2 Fraction of time in different conditions

Vessel type	Bulk carriers larger than Panamax	Panamax bulk carriers and smaller	Vessel intend to carry ore cargoes mostly	Ore carrier
Alternate condition	0.25	0.0	0.5	0.0
Homogenous condition	0.25	0.5	0.0	0.5
Ballast condition	0.35	0.35	0.35	0.35

The fatigue hot spot is always located at the stress concentration zone. The stress concentration factors should be multiplied by the calculated normal stress to obtain

the hot spot stress for the fatigue assessment of the stiffened plate subject to axial and lateral loads. For the fatigue hot spot at the weld connection area between the supporting members and the stiffener flange, the stress concentration factors are listed in table 3. For the hot spot at the mid-span of the plate, a concentration factor for ID 32 is recommended.

Table 3 K factor of typical stiffener support,(37)

ID	Connection Type	Point A		Point B	
		K_a	K_b	K_a	K_b
8		1.52	1.67	1.52	1.67
32		1.13	1.14	N/A	N/A

2.3 Multi-objective optimisation

A genetic algorithm is a kind of bionic algorithm in the macro sense. The mechanism imitates the process of creation and evolution of all life and wisdom. The genetic algorithm is based on the laws of biological evolution. Starting from an initial population, after genetic, evolutionary and natural selection, some of the groups are eliminated, and the remaining individuals form new populations. Then the new population will produce offspring populations continuously, at the same time, evolution may produce new individuals due to mutation. This generation and

generation are multiplying and evolving, resulting in an excellent environment-adapted species. Therefore, this algorithm is also called evolutionary algorithm.

A general constrained multi-objective optimisation problem (MOP) is defined: without exception, the following multi-objective optimisation problem models are considered:

General MOP is composed of n variable parameters, m objective functions and k constraints.

$$\min y = F(x) = (f_1(x), f_2(x), \dots, f_m(x)) \quad (2.23)$$

$$\text{subject to } e(x) = (e_1(x), e_2(x), \dots, e_k(x)) \leq 0, x \in \Omega \quad (2.24)$$

where $x = \{x_1, x_2, \dots, x_n\}$

$$y = \{y_1, y_2, \dots, y_m\}$$

Among them, $x \in \Omega, y \in \Lambda, \Omega$ is the decision space, Λ is the objective function space, the objective function space is made up of the value of the objective function. MOP involves two spaces: decision space and objective function space. Usually, the optimized search process takes place in the objective function space.

For performing the multi-objective optimisation problem, NSGA-II (Non-dominated Sorting Genetic Algorithm II) has been chosen. A typical bi-criterion space solution is shown in Figure 1. The employed NSGA-II program and its calculation flowchart are shown in Figure 2.

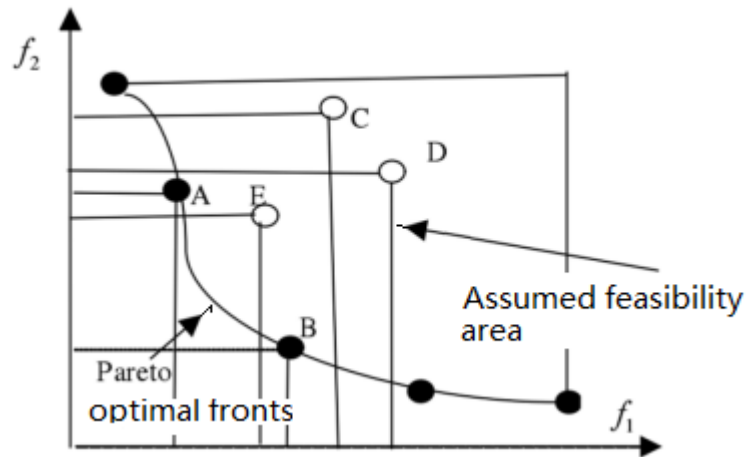


Figure 1 Typical bi-criterion space

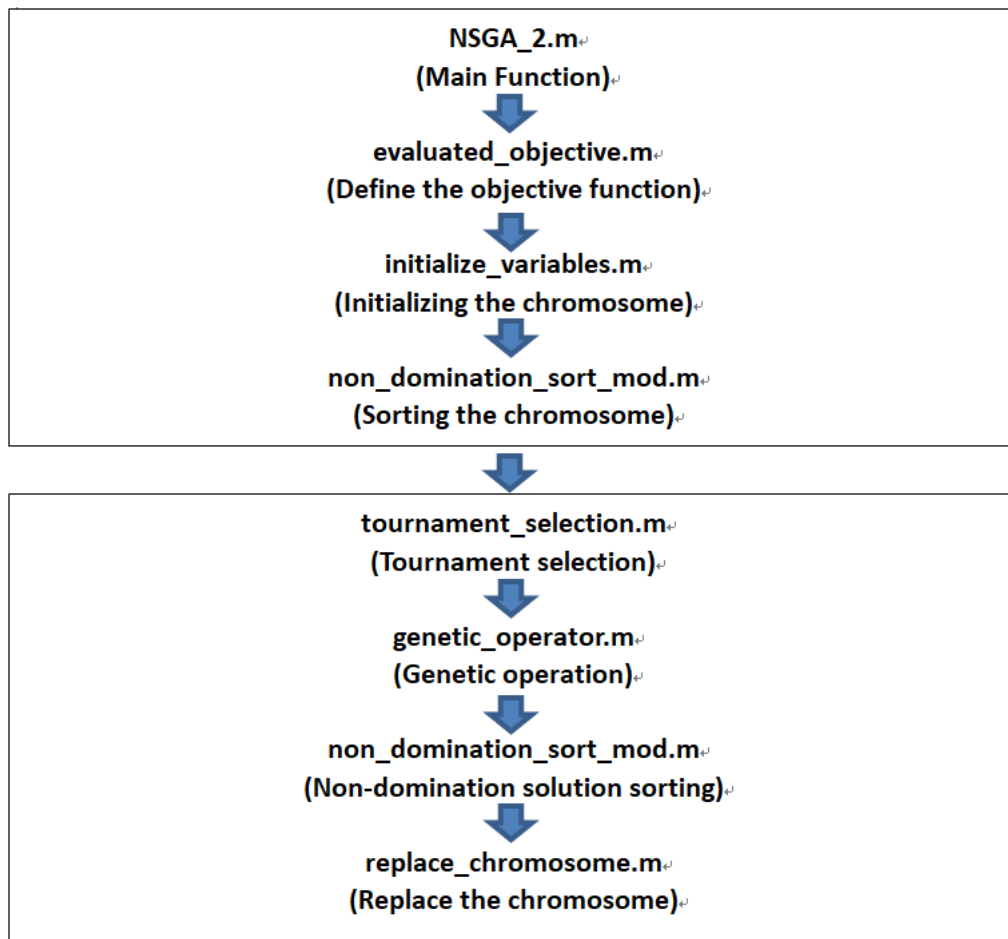


Figure 2 Flowchart of NSGA-II

2.4 Reliability assessment

The JC method is a verification point method based on the first order reliability

methods (FORM) proposed by Hasofer, Lind [42], Rackwitz, and Fiessler [43], Paloheimo and Hannus, [44], which applies to the calculation of structural reliability indicators whose random variables are non-normally distributed. It is easy to understand, and the calculation accuracy can meet the actual needs of the practical application.

It is recommended by the Joint Committee on Structural Safety (JCSS) and is called the JC method.

$P^* (X_1^*, X_2^*, \dots, X_n^*)$ is defined as a checking point (design point), so it is called checking point method. Because it is improved by the central point method, it is called an improved method of the first two moments.

The mathematical derivation is as follows:

Let X_1, X_2, \dots, X_n ($i=1, 2, \dots, n$) as the basic variables and they are independent of each other, then the performance function of the limit state is:

$$Z = g(X_1, X_2, \dots, X_n) \quad (2.25)$$

Expanding the limit state Eqn(2.25) by Taylor's Series at point $P^* (X_1^*, X_2^*, \dots, X_n^*)$ and take the first degree, the limit state Eqn can be expressed as:

$$Z = g(X_1^*, X_2^*, \dots, X_n^*) + \sum_{i=1}^n \frac{\partial g}{\partial X_i^*} \bigg|_{P^*} (X_i - X_i^*) = 0 \quad (2.26)$$

Define $X_i^* = \frac{X_i - \mu_{X_i}}{\sigma_{X_i}}$, then

$$\frac{\partial g}{\partial X_i^*} = \frac{\partial g}{\partial X_i} \frac{\partial X_i}{\partial X_i^*} = \frac{\partial g}{\partial X_i} \sigma_{X_i} \quad (2.27)$$

Replace the Eqn (3-27) into Eqn (3-26); we obtained Eqn (3.28):

$$Z = g(X_1^*, X_2^*, \dots, X_n^*) + \sum_{i=1}^n \frac{\partial g}{\partial X_i^*} \bigg|_{P^*} (X_i - X_i^*) \sigma_{X_i} = 0 \quad (2.28)$$

Mean value:

$$\mu_Z = E(Z) = g(X_1^*, X_2^*, \dots, X_n^*) + \sum_{i=1}^n \frac{\partial g}{\partial X_i^*} \bigg|_{P^*} [E(X_i) - X_i^*] \sigma_{X_i} \quad (2.29)$$

The checking point is on the limit boundary, that is

$$g(X_1^*, X_2^*, \dots, X_n^*) = 0 \quad (2.30)$$

Replace $E(X_i) = \mu_{X_i}$ and Eqn (2.30) in Eqn (3-29),

$$\mu_Z = \sum_{i=1}^n \frac{\partial g}{\partial X_i} \bigg|_{p^*} (\mu_{X_i} - X_i^*) \sigma_{X_i} \quad (2.31)$$

Standard deviation:

$$\sigma_Z = \left[\sum_{i=1}^n \left(\frac{\partial g}{\partial X_i} \bigg|_{p^*} \sigma_{X_i} \right)^2 \right]^{1/2} \quad (2.32)$$

Reliability index:

$$\beta = \frac{\mu_Z}{\sigma_Z} = \frac{\sum_{i=1}^n \frac{\partial g}{\partial X_i} \bigg|_{p^*} (\mu_{X_i} - X_i^*) \sigma_{X_i}}{\left[\sum_{i=1}^n \left(\frac{\partial g}{\partial X_i} \bigg|_{p^*} \sigma_{X_i} \right)^2 \right]^{1/2}} \quad (2.33)$$

If the random variables satisfy the normal distribution:

$$\frac{X_i - \mu_{X_i}}{\sigma_{X_i}} = X_i^* = \beta \cos \theta_{X_i^*} \quad (2.34)$$

$$X_i = \mu_{X_i} + \beta \cos \theta_{X_i^*} \sigma_{X_i} \quad (2.35)$$

Where:

$$\cos \theta_{X_i^*} = \frac{-\frac{\partial g}{\partial X_i} \bigg|_{p^*} \sigma_{X_i}}{\left[\sum_{i=1}^n \left(\frac{\partial g}{\partial X_i} \bigg|_{p^*} \sigma_{X_i} \right)^2 \right]^{1/2}} \quad (2.36)$$

If the random variable does not satisfy the normal distribution, the JC method uses the equivalent normalisation to deal with the problem. The original non-normal distribution variable \mathbf{X}_i is replaced by the equivalent normal distribution, which

satisfies the following two conditions:

- (1) The initial value of the function $F(x_i^*)$ is equivalent to the equivalent normal function value $F'(x_i^*)$.
- (2) The original probability density value $f(x_i^*)$ is equivalent to the equivalent normal distribution probability density value $f'(x_i^*)$.

The mathematical expressions of conditions (1) and (2) above are:

$$F_{X_i'}(x_i^*) = F_{X_i'}(x_i^*) \quad (2.37)$$

$$f_{X_i'}(x_i^*) = f_{X_i'}(x_i^*) \quad (2.38)$$

Eqn (2.37) can be expressed as Eqn (2.39),

$$F_{X_i'}(x_i^*) = \Phi \left(\frac{x_i^* - \mu_{X_i'}}{\sigma_{X_i'}} \right) \quad (2.39)$$

Eqn (2.38) can be expressed as Eqn (2.40),

$$f_{X_i'}(x_i^*) = \frac{dF_{X_i'}(x_i^*)}{dX_i} = \frac{d\Phi \left(\frac{x_i^* - \mu_{X_i'}}{\sigma_{X_i'}} \right)}{dX_i} = \phi \left(\frac{x_i^* - \mu_{X_i'}}{\sigma_{X_i'}} \right) \frac{1}{\sigma_{X_i'}} \quad (2.40)$$

$$\frac{x_i^* - \mu_{X_i'}}{\sigma_{X_i'}} = \Phi^{-1} \left[F_{X_i'}(x_i^*) \right] \quad (2.41)$$

$$f_{X_i'}(x_i^*) = \phi \left[\Phi^{-1} \left(F_{X_i'}(x_i^*) \right) \right] \frac{1}{\sigma_{X_i'}} \quad (2.42)$$

$$\mu_{X_i'} = x_i^* - \Phi^{-1} \left[F_{X_i'}(x_i^*) \right] \sigma_{X_i'} \quad \sigma_{X_i'} = \frac{\phi \left[\Phi^{-1} \left(F_{X_i'}(x_i^*) \right) \right]}{f_{X_i'}(x_i^*)} \quad (2.43)$$

The reliability calculation flowchart is shown in Figure 3.

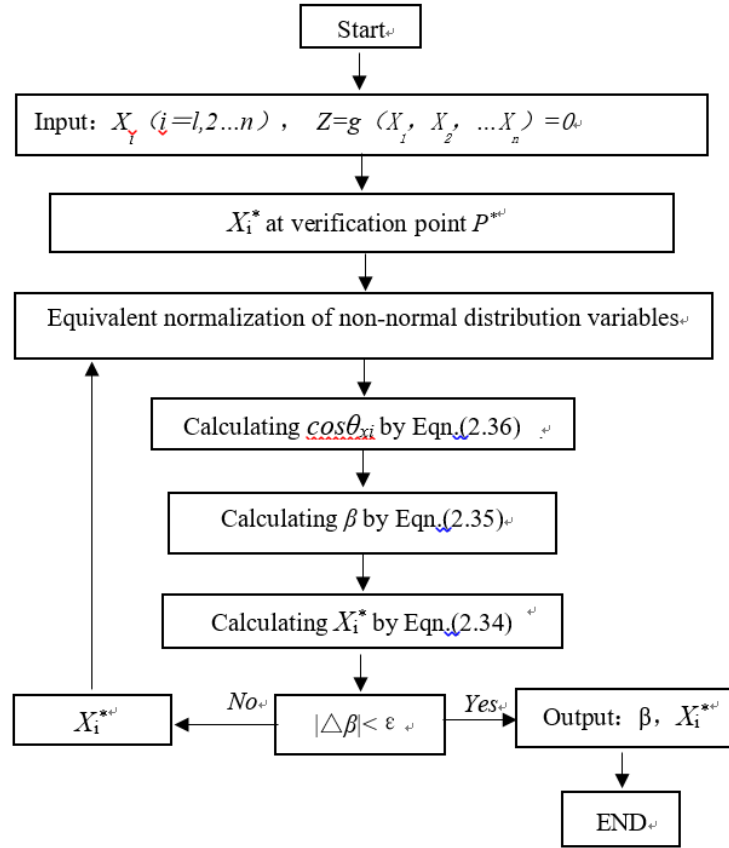


Figure 3 Flowchart of reliability calculation

2.5 Summary

In this chapter, some fundamental theories needed in the optimisation analysis, such as the analysis of a beam under Complex Loading; Fatigue cumulative damage calculation; Basic theory of Multi-Objective Optimization, The specific operation mode of the NSGA-II method and the verification point method of the first order moment theory were introduced.

Chapter 3 Ultimate strength of bulk carrier

3.1 Basic parameters

A 175,000 ton bulk carrier is selected as a target ship. The principal dimensions of the bulk carrier are:

The length between the perpendiculars: $L = 289$ m

Depth: $D = 24.7$ m

Breadth: $B = 45$ m

Design Draft: $d = 18$ m

Block Coefficient: $C_b = 0.79$

The cross-section of the hull girder of this bulk carrier is shown in Figure 4. This cross section contains a total of 129 plates and 98 stiffeners. Longitudinal stiffened plate of a tee-bar profile, with a stiffener spacing 860 mm and frame spacing 2,950 mm, is analysed in the present study.

Geometrical characteristics of the analysed stiffened panels, the dimensional range of plate and stiffener, and their combinations should include most of the realistic member of ship structures. Considering the geometrical characteristics of the bulk carrier, the plate and stiffener are shown in Figure 4. The details of the longitudinal stiffeners are summarised in Table 4, and the material properties are listed in Table 5 respectively.

Table 4 Dimensions of the longitudinal stiffeners of the bulk carrier

No.	Dimensions (mm)	Type	Y.S. (MPa)
1	200 × 20	Flat bar	320
2	150 × 18	Flat bar	320
3	250 × 25	Flat bar	320
4	200 × 20	Flat bar	320
5	420 × 12 + 100 × 20	Tee-bar	320
6	420 × 12 + 100 × 30	Tee-bar	320
7	320 × 12 + 100 × 18	Tee-bar	320
8	300 × 12 + 100 × 12	Tee-bar	320
9	300 × 12 + 100 × 16	Tee-bar	320
10	350 × 12 + 100 × 20	Tee-bar	360
11	300 × 12 + 100 × 18	Tee-bar	360

12	300 × 30	Flat bar	360
13	200 × 20	Flat bar	360
14	350 × 30	Flat bar	360
15	300 × 12 + 100 × 24	Tee-bar	360

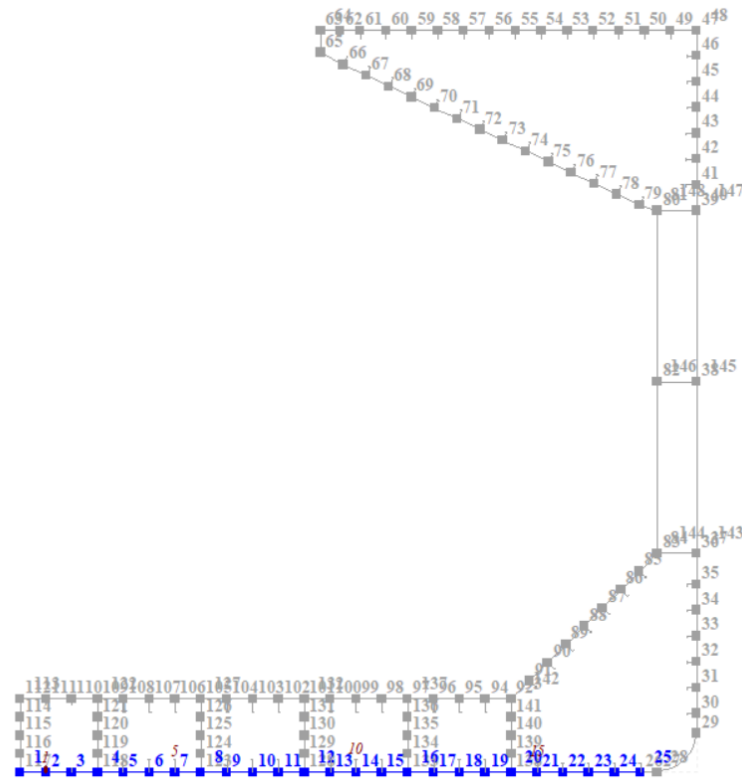


Figure 4 Cross section of the Capesize bulk carrier

Table 5 Material properties of the bulk carrier

	1	2	3
Young's modulus (N/mm ²)	2.1×10^5	2.1×10^5	2.1×10^5
Poisson ratio	0.3	0.3	0.3
Yielding stress (N/mm ²)	235	320	360

3.2 Ultimate strength approach

The hull girder ultimate bending moment capacity, M_u is defined as the maximum bending capacity of the hull girder beyond which the hull will collapse. Hull girder failure is controlled by buckling, ultimate strength and yielding of longitudinal structural elements.

The sagging hull girder ultimate capacity of a hull girder section is defined as the maximum value on the static non-linear bending moment-curvature relationship $M-\kappa$, as can be seen in Figure 5. The curve represents the progressive collapse behaviour of the hull girder under the vertical bending moment.

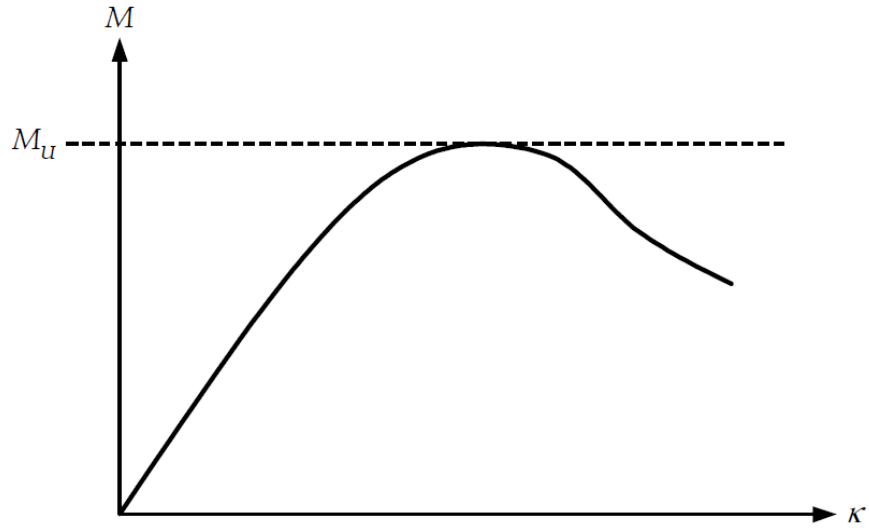


Figure 5 The Bending moment-curvature

The curvature of the critical inter-frame section, κ , is defined by Eqn (3.1).

$$\kappa = \frac{\vartheta}{l} \quad (3.1)$$

Where:

ϑ the relative angular rotation of the two neighbouring cross-sections at transverse frame positions

l the transverse frame spacing, i.e. the span of longitudinals

Incremental-iterative procedure

The most generally used method to assess the hull girder ultimate moment capacity is to derive the non-linear moment-curvature relationship, $M-\kappa$, by incrementally increasing the bending curvature, κ , hull section between two adjacent transverse frames and then identifying the maximum moment along this curve as the ultimate bending capacity, M_u .

The $M-\kappa$ curve is to be based on the axial non-linear $\sigma-\epsilon$ (stress-strain)

load-shortening curves for an individual structural component in the cross-section. The σ - ε curves shall consider all relevant structural effects as listed in Part 1 Chapter 5 Appendix 2 of the Common Structural Rules for bulk carriers and oil tankers [39]. Flow chart of the procedure for the evaluation of the Curve M - k is shown in Figure 6.

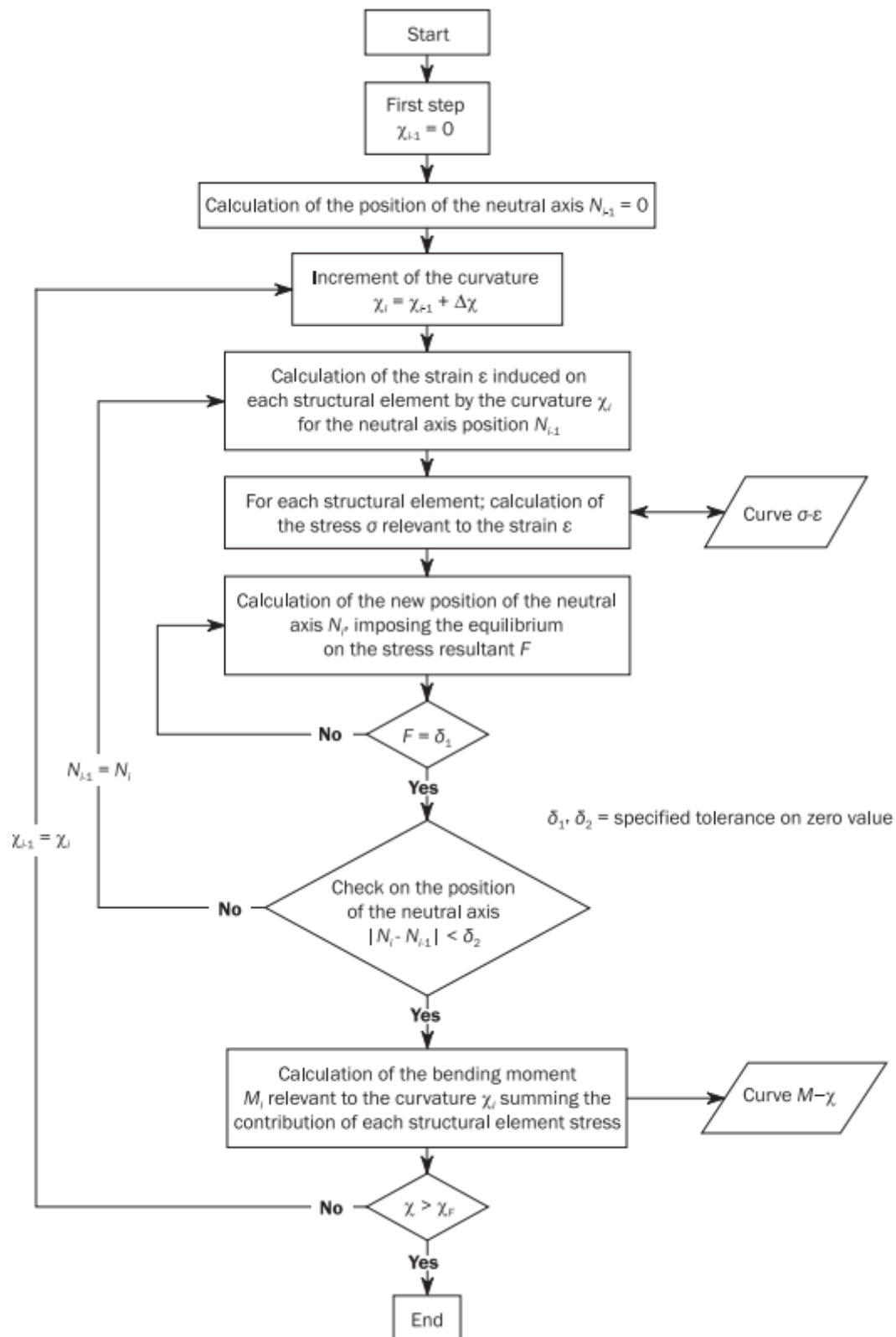


Figure 6 Flowchart procedure for assessment of M-k

3.3 Ultimate strength assessment

The calculation method used here is using the software Mars2000 [51]. By attributing all information about the cross-section, which includes the position, shape and properties of all nodes, plates and stiffeners, the geometric properties, hull girder strength criteria can be calculated here. The target ship is a 175,000 ton bulk carrier, half of its middle section is shown in Figure 7. The calculated hull girder loads are shown in Figure 8. The estimated geometric properties of the compute sectional area are shown in Figure 9. The calculated section module and the rule required values were shown in Figure 10. The calculated ultimate strength of the hull girder is shown in Figure 11.

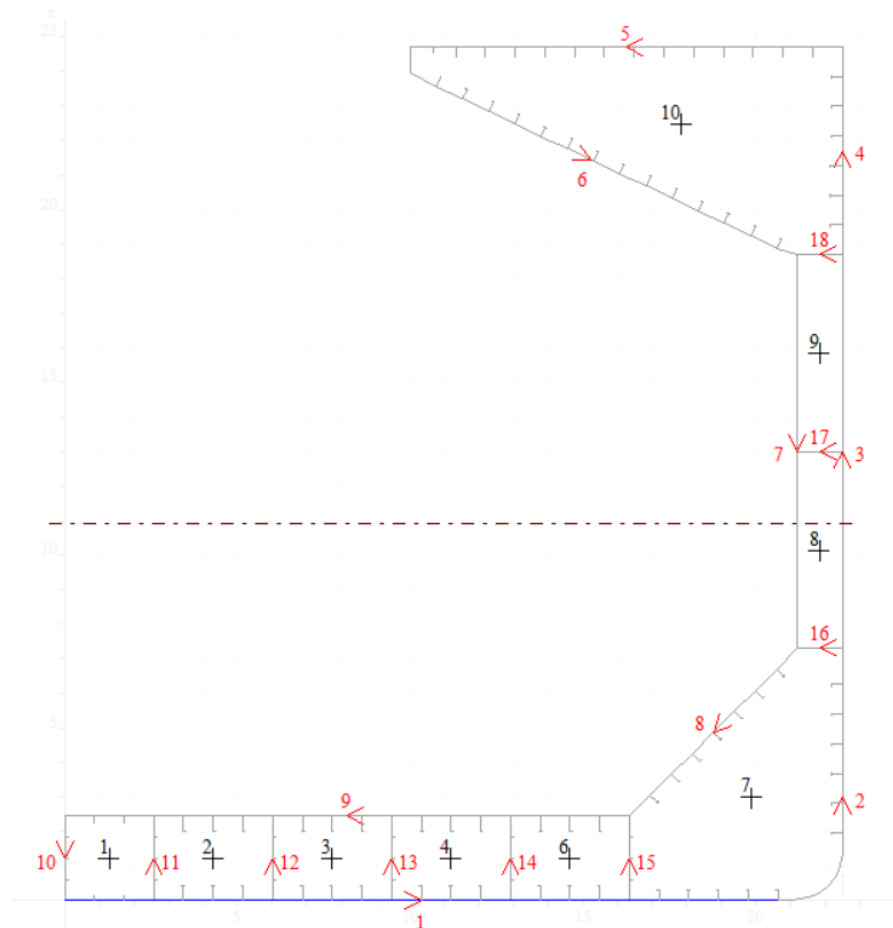


Figure 7 Geometric properties of sectional area

Hull girder strength criteria

Hull Girder Loads | Section Moduli | Ultimate Strength | Net/Gross Moduli

	Hogging	Sagging	
Design S.W.B.M. (still water bending moment)	4 455 451.	- 3 899 778.	(kNm)
Design vertical wave bending moment (rule)	6 043 952.	- 6 599 625.	(kNm)
Rule horizontal wave bending moment	0.		(kNm)
	Positive	Negative	
Design vertical shear force	100 000.		(kN)
Rule vertical wave shear force	43 596.	- 43 596.	(kN)

Close

Figure 8 Calculated hull girder loads

Geometric Properties

☒ Gross scantling ☐ Net scantling

Full section | Half section

Gross area of cross-section	6.02854	m ²
Effective area of cross-section	6.02854	m ²
Moment of inertia / GY axis	603.2371	m ⁴
Moment of inertia / GZ axis	1618.6791	m ⁴
Neutral axis (above base line)	10.903	m
Section modulus at deck (Wp)	43.7236	m ³
Section modulus at bottom (Wf)	55.3256	m ³

Reference Young Modulus = 206000 Mpa

Figure 9 Calculated geometric properties of sectional area

Hull girder strength criteria

Hull Girder Loads | **Section Moduli** | Ultimate Strength | Net/Gross Moduli

	Rule	Actual	at z / BL
Modulus at deck	42.85471	43.72359 (m3)	24.700 (m)
Modulus at bottom	46.34736	55.32560 (m3)	0.000 (m)
Inertia	520.17040	603.23710 (m4)	

Close

Figure 10 Calculated section module and rule required values

Hull girder strength criteria

Hull Girder Loads | Section Moduli | **Ultimate Strength** | Net/Gross Moduli

Ultimate Bending Capacity (kN.m)
Calculated with net scantling (with corrosion margin x 1.000)

	Mu		Ultimate	Mb	z	
Hogging	15 012 460.	Navigation	14 289 420.	11 103 800.	77.71	Hogging
Sagging	- 14 265 420.		- 13 578 360.	- 11 159 370.	82.18	Sagging

The hull girder ultimate bending moment capacity is calculated with a code developed by the Technical University of Szczecin

Close

Figure 11 Calculated ultimate strength of hull girder

3.4 Summary

In this chapter, the necessary parameters of the target ship were first introduced, the calculation procedure of ultimate strength of ship hull was showed after it, then a 175,000ton bulk carrier is as the target ship and its ultimate strength was calculated by using software MARS2000. The calculated results will be used as input data in the optimisation analysis of the stiffened plate in the bottom of the ship in the following chapter.

Chapter 4 Optimization of bottom stiffened plate

4.1 Basic parameters of selected stiffened plate

For bulk carriers in hogging, the most critical situation is the alternate hold loading (AHL) condition with odd-numbered holds loaded with high-density cargoes and even-numbered holds empty. The effect of the local lateral pressure should be considered in the assessment of ultimate hull girder strength in the hogging and AHL conditions. In the present study, the ultimate strength of a Capesize bulk carrier hull girder under combined global and local loads in the hogging and AHL condition is investigated following the DNV rules [45].

The position of the stiffened plate selected for optimisation is on the bottom plate of the ship, which has coordinates of the weld position of the specified stiffener as (3.44, 0). The transverse distance from the middle of the ship is 3.44 m, and the horizontal height is 0 m. The stiffener type of this position is T-bar. The thickness of its adjacent bottom plates is 18 mm on both sides of it. The original geometric parameters of the stiffened plate are shown in Table 6. The geometry parameters of the specific plate are shown In Figure 13.

Structural member: Double bottom longitudinal;

Structural detail: Connection to transverse webs and bulkheads;

Load type: Hull girder is bending stress, double bottom bending stress and sea-, cargo- and ballast pressure load.

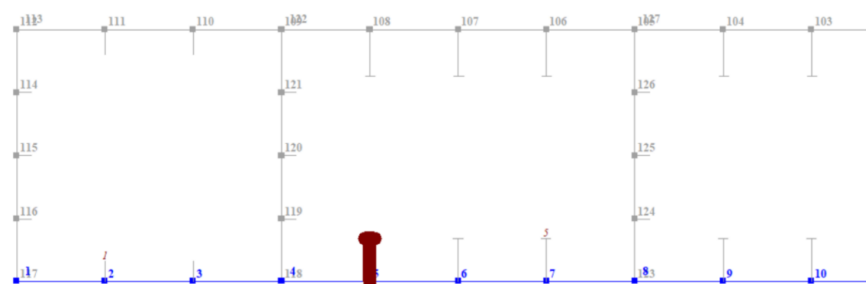


Figure 12 Longitudinal in bulk carrier

Table 6 Original geometric parameters of stiffened plate

Width of the bottom plate, s	860	mm
Web height, h_w	420	mm
Web thickness, t_w	12	mm
Flange Breadth, b_f	100	mm
Flange thickness, t_f	20	mm

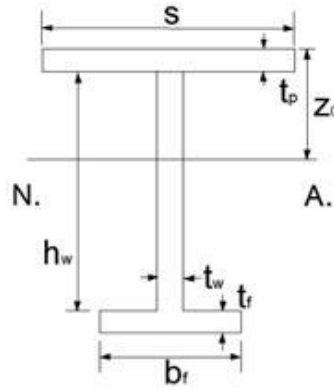


Figure 13 T-type stiffened plate cross section diagram

The formula (4.1) and (4.2) are used for calculating the Inertia moment and the position of the Neutral axis of the stiffened plate.

$$I = \int_A z^2 dA = \sum (I_i + z_{ic}^2 A_i) \quad (4.1)$$

$$z_c = \frac{\sum z_i A_i}{\sum A_i} \quad (4.2)$$

$$I = \frac{St_p^3}{12} + St_p(z_0 - \frac{t_p}{2})^2 + \frac{t_w h_w^3}{12} + h_w t_w (z_0 - t_p - \frac{h_w}{2})^2 + \frac{b_f t_f^3}{12} + b_f t_f (z_0 - t_p - h_w - \frac{t_f}{2})^2 \quad (4.3)$$

$$z_c = \frac{St_p^2 / 2 + t_w h_w (t_p + h_w / 2) + t_f b_f (t_p + h_w + t_f / 2)}{St_p + t_w h_w + t_f b_f} \quad (4.4)$$

4.2 Loads on stiffened plate

The wave-induced bending moments in hogging and sagging are given according to DNV rule, and the distribution factor F_M is depending on the ship length shown in Table 7.

Table 7 Distribution factor F_M

<i>Hull transverse section location</i>	<i>Distribution factor F_M</i>
$0 \leq x < 0.4L$	$2.5 \frac{x}{L}$
$0.4L \leq x \leq 0.65L$	1.0
$0.65L < x \leq L$	$2.86 \left(1 - \frac{x}{L}\right)$

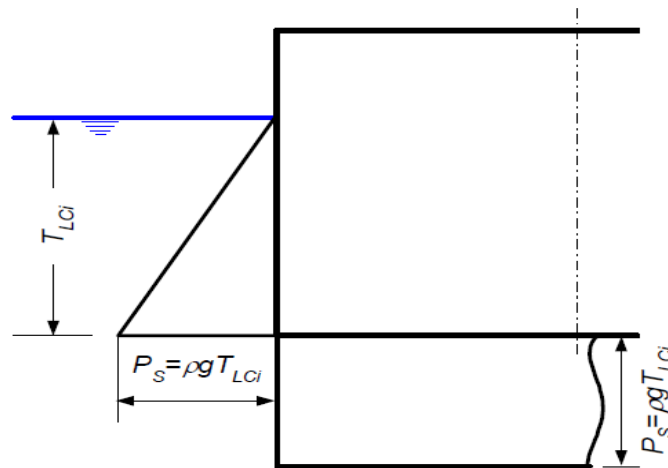


Figure 14 Local static and dynamic pressure loads

Wave-induced bending moments in hogging and sagging conditions are:

$$M_{w,h}^{CSR} = 190 F_M f_p C L^2 B C_b 10^{-3} \quad (4.5)$$

$$M_{w,s}^{CSR} = -110 F_M f_p C L^2 B (C_b + 0.7) 10^{-3} \quad (4.6)$$

Still water bending moments in hogging and sagging conditions.

$$M_{sw,h}^{CSR} = 175 C L^2 B (C_b + 0.7) 10^{-3} - M_{w,h}^{CSR} \quad (4.7)$$

$$M_{sw,s}^{CSR} = -175 C L^2 B (C_b + 0.7) 10^{-3} - M_{w,s}^{CSR} \quad (4.8)$$

The local static and dynamic pressure loads are shown in Figure 14 and calculated by using Eqns (4.9)-(4.12).

Full load condition:

$$P_{sw}^{CSR} = \rho g T_{LCi} \quad (4.9)$$

Where:

$$p_{HF} = 3f_p f_{nl} C \sqrt{\frac{L+\lambda-125}{L}} \left(\frac{z}{T_{LCi}} + \frac{|2y|}{B_i} + 1 \right) \quad (4.10)$$

With $\frac{|2y|}{B_i} \leq 1.0$ and z is to be taken not greater than T_{LCi}

λ = Wave length, in m, taken equal to:

$$\lambda = 0.6 \left(1 + \frac{T_{LC}}{T_S} \right) L \quad \text{for load cases H1 and H2}$$

$$\lambda = 0.6 \left(1 + \frac{2 T_{LC}}{3 T_S} \right) L \quad \text{for load cases F1 and F2}$$

$$P_w^{CSR} = 3f_p f_{nl} C \sqrt{\frac{L+\lambda-125}{L}} \left(\frac{z}{T_{LCi}} + \frac{|2y|}{B_i} + 1 \right) \quad (4.11)$$

Ballast Load condition:

$$P_{sw}^{CSR} = \rho g T_{LCi} \quad (4.12)$$

$$P_w^{CSR} = 3f_p f_{nl} C \sqrt{\frac{L+\lambda-125}{L}} \left(\frac{z}{T_{LCi}} + \frac{|2y|}{B_i} + 1 \right) \quad (4.13)$$

The inertia moment of the midship net section concerning the neutral axis is shown in Figure 9:

$$I_{na} = 603.2371 \text{ m}^4$$

Moreover, the midship section modulus concerning the bottom line is shown in Figure 9:

$$W_b = 55.3256 \text{ m}^3$$

The yield strength is $\sigma_y = 315 \text{ MPa}$ and the Young modulus is $E = 210 \text{ GPa}$.

The span of the longitudinal stiffener (stiffened plate) is $L = 2950 \text{ mm}$

The distance between the longitudinal stiffeners is $b_p=860$ mm

The geometry parameters in Table 6 will be defined during the optimisation process.

The studied longitudinal stiffener is subjected to axial stresses resulting from the vertical still water and wave-induced bending moments [35]:

$$\sigma_{global} = \frac{M_{sw} + \Psi M_w}{W_{bottom\ ship}} \quad (4.14)$$

$$\sigma_{global} = \frac{M_{sw} + \Psi M_w}{W_{bottom\ ship}}$$

Where Ψ is a combination factor between the still water and wave-induced loads ranging from 0.8 to 0.95 depending on the assumptions, and it is assumed here to be a deterministic one of 0.9. The stiffener plate is also subjected to a lateral load, induced by the hydrostatic and dynamic local pressure,

$$q_{local} = (P_{sw} + \Psi P_w) b_p \quad (4.15)$$

Full load condition:

$$q_{local1} = (P_{sw1} + \Psi P_{w1}) b_p$$

Ballast load condition:

$$q_{local2} = (P_{sw2} + \Psi P_{w2}) b_p$$

The stiffened plate is assumed to be a simply supported beam subjected to a uniformly distributed lateral load, q_{local} and axial tensile force $T = A(M_{sw,s} + \Psi M_{w,s})/W_{bottom\ ship}$ in the case of sagging loading and to an axial compressive force $T^* = A(M_{sw,h} + \Psi M_{w,h})/W_{bottom\ ship}$ in the case of hogging respectively, where A is the net sectional area of the stiffened plate. In the present study, only the compressive load will be considered in the design of the stiffened plate.

The maximum stresses at the middle of the beam are calculated as:

$$\sigma_{max,x=0} = \sigma_{local} + \sigma_{global} \quad (4.16)$$

Where

$$\sigma_{local}(P_{sw}, P_w) = \frac{m_{x=0}(u^*)}{W_{stiffened\ plate}}$$

$$\sigma_{global}(M_{sw,s}, M_{w,s}) = \frac{M_{sw,s} + \Psi M_{w,s}}{W_{bottom\ ship}}$$

However, due to the local outside water pressure load that is acted on the bottom plate of the ship, the bottom line of the stiffened plate is subjected to axial compressive stresses as calculated by Eqn (4.14).

4.3 Optimization based on weight and fatigue

The goal of the structural design is to find the best dimensions for the three-dimensional structures. Often, this is treated as a single-objective optimisation problem. However, many design problems are multi-state, multi-specificity or otherwise require concurrent optimisation of multiple objectives. There may be tradeoffs among objectives, where improving on feature requires compromising another. The challenge lies in determining solutions that are part of the Pareto optimal set—designs where no further improvement can be achieved in any of the objectives without degrading one of the others. Pareto optimality problems are found in all areas of different studies, and computational methods have been developed specifically to identify the Pareto frontier.

A genetic algorithm with termination criteria is employed here defined as a non-dominated sorting generic algorithm, NSGA-II developed by Deb et al. (2002) in determining the best design solutions of the stiffened plate subjected to compressive loading.

The objective functions and the constraints, involving the design variables, are nonlinearly resulting in a non-linear optimisation problem. Five steps in the genetic algorithm are shown in figure 2.2 and included in the following steps.

- 1 – generation of the initial population,

- 2 – sorting the population based on the Pareto non-domination criteria,
- 3 – evaluation of any individual fitness according to the Pareto ranking,
- 4 – parent selection based on individual fitness,
- 5 – application of genetic operators to generate a new population,
- 6 – identifying the best non-dominated solution and finally,
- 7 – verifying the convergence and found ends the process otherwise return to Step 3.

The genetic algorithm NSGA-II stops when it cannot accommodate into a non-dominated solution set.

4.3.1 Decision variables

In this study there are five decision variables considered that determine the shape of the cross-sectional area. Choosing the appropriate range of the value of the decision variables is a fundamental issue. The appropriate range can make it easier to get results that meet the specification requirements in the subsequent Pareto frontier calculation.

The decision variables assumed here are $x_1 = t_p$, $x_2 = h_w$, $x_3 = t_w$, $x_4 = b_f$, $x_5 = t_f$,

$$x = \{x_1, x_2, x_3, x_4, x_5\}^{-1} \quad (4.17)$$

And their range is defined as:

$$x_{i,\min} \leq x_i \leq x_{i,\max}, i \in [1,5] \quad (4.18)$$

The original dimensions of the stiffened plate with its attached plate considered here is $t_p = 0.018 \text{ m}$, $b_f = 0.1 \text{ m}$, $t_f = 0.02 \text{ m}$, $h_w = 0.42 \text{ m}$, $t_w = 0.012 \text{ m}$. Since the optimal design is based on this model, the dimensions of the decision variables will not change too much. So it can be used as a reference for the definition of the new ranges of the variables. Then after some trial operations, the final definitions of the variable ranges are as follows:

Where:

$$x_{1,min} = 0.012 \text{ m}, x_{1,max} = 0.03 \text{ m}$$

$$x_{2,min} = 0.4 \text{ m}, x_{2,max} = 0.5 \text{ m}$$

$$x_{3,min} = 0.012 \text{ m}, x_{3,max} = 0.03 \text{ m}$$

$$x_{4,min} = 0.1 \text{ m}, x_{4,max} = 0.2 \text{ m}$$

$$x_{5,min} = 0.012 \text{ m}, x_{5,max} = 0.03 \text{ m}$$

min_range_of_decision_variable=[0.012,0.4,0.012,0.1,0.012];

max_range_of_decision_variable=[0.03,0.5,0.03,0.2,0.03];

4.3.2 Objective Functions

There are three critical factors in this situation that need to be taken into consideration, so there are three objective functions need to be built.

All of them need to meet the requirement of the classification society rules.

The two-objective structural responses considered is minimising the weight, which leads to minimising of the net sectional area and minimising the structural displacement, which defines a multi-objective optimisation problem:

$$F_1 = \min\{z_{x=0}(b, x)\} \quad (4.19)$$

$$F_2 = \min\{A(b, x)\} \quad (4.20)$$

Where $z_{x=0}(b, x)$ is the displacement at the middle of the span and $A(b, x)$ is the net-sectional area of the stiffened plate, $b = \{\sigma_y, E\}^{-1}$ is for the material properties.

The third objective function is to minimizing the cumulative damage.

$$F_3 = \min\{D_{x=0}(b, x)\} \quad (4.21)$$

4.3.3 Constraints

The dimensions of the flange, web and attached plate of the stiffened plate have to

satisfy the following constraints:

$$G_1: x_1 - \frac{b_p}{c} \sqrt{\frac{\sigma_y}{235}} > 0 \quad (4.22)$$

$$G_2: x_3 - \frac{h_w}{c_w} \sqrt{\frac{\sigma_y}{235}} > 0 \quad (4.23)$$

$$G_3: x_5 - \frac{b_f}{c_f} \sqrt{\frac{\sigma_y}{235}} > 0 \quad (4.24)$$

Where b_p is the space defined as a distance between the longitudinal stiffeners, $C=100$, $C_w = 75$, $C_f = 12$ (IACS).

The type of load subjected to the stiffened plate will induce the plate buckling since the stiffener is subjected to a tensile load and the attached plate to a compressive load. Some variables for the optimisation are listed in Table 8

Table 8 Two loading conditions and fraction of time

Load Condition		Fraction of time
Full load	Sagging	0.5
Ballast	Hogging	0.35

Table 9 The still water and wave-induced bending moments

	Sagging	Hogging	
$M_{SW,CS}$	-3899778.069	4455451.144	kN.m
$M_{W,CS}$	-6599624.424	6043951.348	kN.m

Table 10 The Weibull shape factor and the reference period and wave

$h_{Weibull}$	0.931	-
$T_{reference}$	1	year
T_{wave}	8	sec

4.4 Reliability-based design optimisation

The empirical formula for the assessment of the load carrying capacity of the stiffened panel would be more useful for the design [46] and the reliability analysis of ship structure, although the factors of safety in association with uncertainties and deviations should be considered carefully [35]. The reliability analysis performed

here is using the FORM techniques that identify a set of basic random variables, which influence the limit-state under consideration. The limit-state function defines a failure surface when equals to 0, which is, in fact, an (n-1) dimensional surface in the space of n basic variables. The formation of RBDO is similar to the one of the optimisations where the objective limits state function, $g(b,x)$ is minimised, and it is subject to constraints, where b is the vector of the deterministic design variables and x is the vector of the random variables. The limit state function here is defined as [35]:

$$g(b,x) = \sigma_u(b,x) - \sigma_{\max}(b,x) \quad (4.24)$$

Where

$$\sigma_{\max}(b,x) = \sigma_{\text{global,max}}(b,x) + \sigma_{\text{local,max}}(b,x) \quad (4.25)$$

$$\sigma_{\text{global,max}}(b,x) = k_1(X_{m,sw}M_{sw} + \Psi X_{m,w}M_w) / W_b \quad (4.26)$$

$$\sigma_{\text{local,max}}(b,x) = m_{x=0}(u^*) / W_{b,stiff} = k_2(X_{p,sw}P_{sw} + \Psi X_{p,w}P_w)l / W_{b,stiff} \quad (4.27)$$

This surface divides the basic variable space in a safe region, where $g(b,x) > 0$ and an unsafe area where $g(b,x) < 0$. The failure probability of a structural component concerning a single failure mode can formally be written as:

$$P_f = P[g(b,x) \leq 0] \quad (4.28)$$

Where P_f denotes the probability of failure. In practical applications, the FORM methods provide a way of evaluating the reliability efficiently with reasonably good accuracy [35].

The required safety index is defined here as β_{target} , the Beta index of all feasible design solution, as defined by the Pareto frontier, is compared to the required target safety index, where $\min\{\beta_{\text{target}} - \beta_i\}$ is the best reliability based design solution.

Seven deterministic variables are considered here as [35]: $b_1 = t_p$, $b_2 = h_w$, $b_3 = t_w$, $b_4 = b_f$, $b_5 = t_f$, $b_6 = \sigma_y$, $b_7 = E$, and ten random variables $x_1 = M_{w,BL,hog}$, $x_2 = P_{w,BL,h}$, $x_3 = M_{sw,BL,h}$, $x_4 = P_{sw,BL,h}$, $x_5 = \sigma_u$, $x_6 = X_u$, $x_7 = X_{p,sw}$, $x_8 = X_{m,sw}$, $x_9 = X_{p,w}$, $x_{10} = X_{m,w}$, are considered here, where

$$x = \{M_{w,BL,hog}, P_{w,BL,h}, M_{sw,BL,h}, P_{sw,BL,h}, \sigma_u, X_u, X_{p,sw}, X_{m,sw}, X_{p,w}, X_{m,w}\}^{-1} \quad \text{and} \\ b = \{t_p, h_w, t_w, b_f, t_f, \sigma_y, E\}^{-1}.$$

The local lateral load is defined as $q_{local} = (X_{p,sw}P_{sw,BL,h} + \Psi X_{p,w}P_{w,BL,h})b$ and the net sectional stresses, resulting from the global bending load, is $\sigma_{global} = (X_{m,sw}M_{sw,BL,h} + \Psi X_{m,w}P_{w,BL,h})/W_b$. σ_u is the ultimate stress capacity with a model uncertainty factor X_u , which is assumed to be described by the Normal probability density function, $N_{x,u}(1.05,0.1)$.

The model uncertainty factor $X_{m,w}$ accounts for the uncertainties in the wave induced vertical bending moment calculation. Resulting in $X_{m,w} \sim N_{x,m,w}(1,0.1)$ and the model uncertainty factor with respect to the still water load is $X_{m,sw} \sim N_{x,m,sw}(1,0.1)$ and with respect to the local pressure load are modelled by $X_{p,sw} \sim N_{p,sw}(1,0.1)$ and $X_{p,w} \sim N_{p,w}(0.95,0.095)$.

The fraction of time spent in each load condition may be estimated based on the statistical analysis of the operational profile of the bulk carrier ship. The assumed operational profile here is a full load, $p_{FL} = 0.5$, ballast load, $p_{BL} = 0.35$. The vertical wave-induced bending moment is in sagging in the full loading condition and in hogging in ballast and partial loading conditions. The still water bending moment is in sagging in full loading condition and in hogging in ballast and partial loading conditions. The ballast loading case is used in the present analysis since it transmits a compressive load to the stiffened plate at the bottom of the ship.

The still water bending moment is fitted to a Normal distribution. The regression Eqns define the statistical descriptors of the still water bending moment as a function of the length of the ship, $W=(DWT/Full \text{ load})$ as proposed by Guedes Soares and Moan[47], Guedes Soares [48] and the loads are taken as prescribed by the Classification Societies Rules [39].

4.4.1 Ultimate bending moment

The 5% confidence level value of the ultimate bending moment $M_u^{5\%} = M_u^c$ is calculated by MARS2000 software and it is assumed that COV equals to 0.08 and it is fitted to the Lognormal probability density function [35]:

$$f_{Mu} = \frac{1}{M_u \sigma_{Mu} \sqrt{2\pi}} e^{-\frac{(\ln(M_u) - \mu_{Mu})^2}{2\sigma_{Mu}^2}} \quad (4.29)$$

$$\sigma_{Mu} = \sqrt{\ln(COV^2 + 1)} \quad (4.30)$$

$$\mu_{Mu} : F_{Mu}^{-1}(0.05, \mu_{Mu}, \sigma_{Mu}) = M_u^{5\%} \quad (4.31)$$

The ultimate bending moment statistical descriptors are given in Table 11.

Table 11 Statistical parameters of ultimate bending moments

Load Conditions	Mean, MN.m	StDev, MN.m	COV	Distribution	$Mean_{Msu}$	$StDev_{su}$	5%
$M_u(sag)$	15012	1201	0.08	Lognormal	9.699	0.08	14289
$M_u(hog)$	14356	1149	0.08	Lognormal	9.648	0.08	13578

4.4.2 Bending moment load

The Gumbel distribution, for the extreme values of the vertical wave-induced bending moment, over the reference period T_r is derived based on the shape, h and scale, q factors of the Weibull distribution function as [53] :

$$\alpha_m = q(\ln(n))^h \quad (4.32)$$

$$\beta_m = \frac{q}{h} (\ln(n))^{(1-h)/h} \quad (4.33)$$

Where α_m and β_m are the parameters of the Gumbel distribution, n is the mean number of load cycles expected over the reference time period T_r for a given mean value wave period T_w . It is assumed here that $T_r = 1$ year and $T_w = 8$ sec. The mean number of load cycles n is calculated as:

$$n = \frac{pT_r(365)(24)(3600)}{T_w} \quad (4.34)$$

Where p is the partial time in which the ship is in seagoing conditions (full, ballast, partial loads)

The Gumbel distribution function is described as:

$$F_{Mw} = \exp \left\{ -\exp \left(-\frac{M_{w,e} - \alpha_m}{\beta_m} \right) \right\} \quad (4.35)$$

Where $M_{w,e}$ is a random variable that represents the extreme value of the vertical wave-induced bending moment over the reference time period, T_r .

The selected target ship is a bulk carrier larger than Panamax with 175,000 tones. From Table 2, there is three fractions of time for this ship, 0.25 for the Alternate condition, 0.25 for the homogeneous condition, and 0.35 for ballast condition. For simplifying the calculation, the alternate conditioned the homogeneous condition are catalogued into the full load condition. That is:

Full load condition:

$$p_1 = 0.5$$

Ballast condition:

$$p_1 = 0.35$$

The wave-induced vertical bending moment and local dynamic pressure statistical descriptors are given in Table 12 and Table 13.

Table 12 Wave-induced vertical bending moment statistical descriptors

Load conditions	Distribution	Fraction of time	n, cycles	α , MN.m	β , MN.m
FL(sag)	Gumbel	0.5	1971000	3481.821	378.014
BL(hog)	Gumbel	0.35	1379700	3115.534	345.548

Table 13 Wave-induced dynamic pressure statistical descriptors

Load conditions	Distribution	Fraction of time	n, cycles	α , MN.m	β , MN.m
FL(sag)	Gumbel	0.5	1971000	0.02476	0.0026886
BL(hog)	Gumbel	0.35	1379700	0.0242	0.00268

The still water bending moment is fitted to a Normal distribution. Regression Eqns

developed in [54] define the statistical descriptors of the still water bending moment as a function of length, L and dead-weight ratio, $W=(DWT/Full\ load)$, which coefficients are given in Table 14 and the calculated mean and standard deviation of still water bending moment are listed in Table 15.

Table 14 Coefficients for calculating the mean and standard deviation of still water bending moment

Data Set	a_0	a_1	a_2
$Mean(M_{SW,max}) = a_0 + a_1 \cdot W + a_2 \cdot L$	114.7	-105.6	-0.154
$StDev(M_{SW,max}) = a_0 + a_1 \cdot W + a_2 \cdot L$	17.4	-7	0.035

Table 15 Mean and standard deviation of still water bending moment

	FL(sag)	BL(hog)
$Mean(M_{SW,max})$	-24.846	49.074
$StDev(M_{SW,max})$	21.215	26.115

$$Mean(M_{SW}) = \frac{Mean(M_{SW,max})M_{SW,CS}}{100} \quad (4.36)$$

$$StDev(M_{SW}) = \frac{StDev(M_{SW,max})M_{SW,CS}}{100} \quad (4.37)$$

Table 16 Statistical descriptors of still water bending moment

Load conditions	W=DWT/Full Load	Distribution	Mean, MN.m	StDev, MN.m
FL(Sagging)	0.9	Normal	968.939	827.338
BL(Hogging)	0.2	Normal	2186.468	1163.541

4.4.3 Other uncertainty factors

The statistical descriptions of the uncertainty coefficients involved in the limit state function are assumed and listed in Table 17.

Table 17 Statistical descriptors of X

Uncertainty factors	Distribution	Mean	StDev	COV
X_u	Normal	1.05	0.1	0.095
X_{SW}	Normal	1.00	0.1	0.1
X_W	Normal	1.00	0.1	0.1
X_S	Normal	1.00	0.1	0.1

Where denotes the normal distribution function and the first and second indicator inside of the brackets refer to the mean value and standard deviation respectively.

4.5 Analysis

4.5.1 Multi-objective optimisation

The Pareto frontier [49] is employed here allowing for the optimisation of the three criterions, as they are defined in the present study as the minimum net sectional area, displacement and the fatigue damage factor D, verifying all trade-offs among the optimal design solutions of the three criteria.

The multi-objective optimisation was performed by Matlab, and the optimal results are written in a file 'solution.txt'. The 'solution' file contains a series of optimal results, each of them includes the 5 design variables which determine the shape and area of the stiffened plate with their corresponding results of the three objective functions which are sectional area, displacement at the middle of the span and the fatigue damage factor D. The optimization results are listed in Table 13.

Figure 15 shows the minimisation of the two objective functions, F_1 (net sectional area) and F_3 (fatigue damage) simultaneously. Figure 16 shows the minimization of the two objective functions, F_1 (net sectional area) and F_2 (displacement) simultaneously.

The curve in Figure 15 indicates the Pareto optimal frontier, whereby any improvement concerning F_1 comes at the bigger value of F_2 . Each design solution, allocated at that frontier represents unique design solution parameters. The Pareto optimal solution collected here 100 optimal design solutions that are going to be verified with respect to the target reliability in the next section, leading to an additional constraint in the optimization process.

After that the points that do not meet the regulations were deleted, one can move on to the next step, the reliability design.

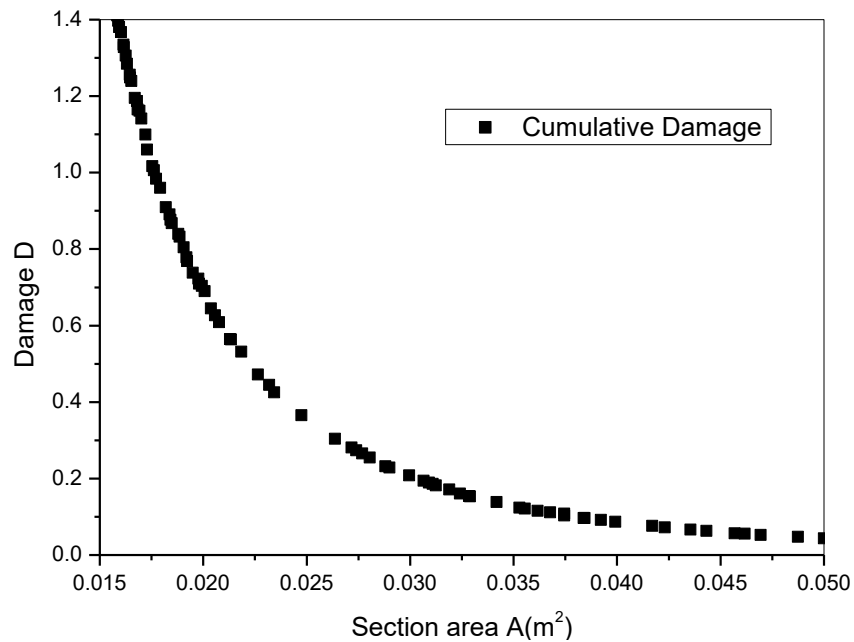


Figure 15 Pareto frontier solution- net section area vs fatigue damage

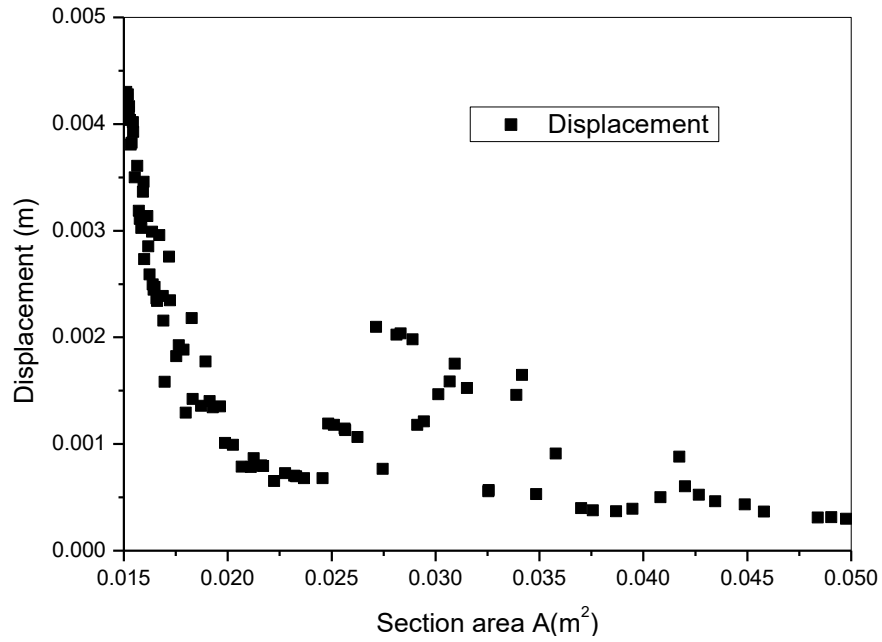


Figure 16 Pareto frontier solution the net section area vs displacement

The results here are not considering the conditional criteria. Then the results are imported in to excel for the next step of selection, where two formulae are used for the judgment process. One is to make sure that the fatigue damage factor D is not more than 1; the other one is to make sure that the optimised sectional area of the stiffened plate is not more significant than the original sectional area.

4.5.2 Reliability-based design optimisation

The reliability analysis is incorporated into the optimisation procedure, which is referred here as reliability-based design optimisation, RBDO. The statistical nature of the constraints and design problems are defined in the objective function including the probabilistic constraints. The probabilistic constraints can specify the required reliability target level.

The reliability is performed based on FORM, and all random variables are considered as non-correlated ones. Applying FORM as a decision tool, the estimated probability of failure needs to be compared to an accepted target level. The target levels depend on different factors as reported by Moan (1998). The target level adapted here, which may result in a redundant structure in $P_f = 10^{-3}$ ($\beta = 3.09$) for less serious

and $P_f = 10^{-4}$ ($\beta = 3.71$) for serious consequences of failure values of the acceptable annual probability of failure [45].

During the buckling check step, the input values of the random variables which describe the two loading conditions were taken into consideration, and so the two kinds of results were obtained. The beta index of the buckling check is the combination of the two situations using the fraction of time of the load condition of the bulk carrier as the weighting coefficient. After that, the result of the buckling check is combined with the results obtained by the fatigue check again. At this point, the probability of the two outcomes is both 0.5.

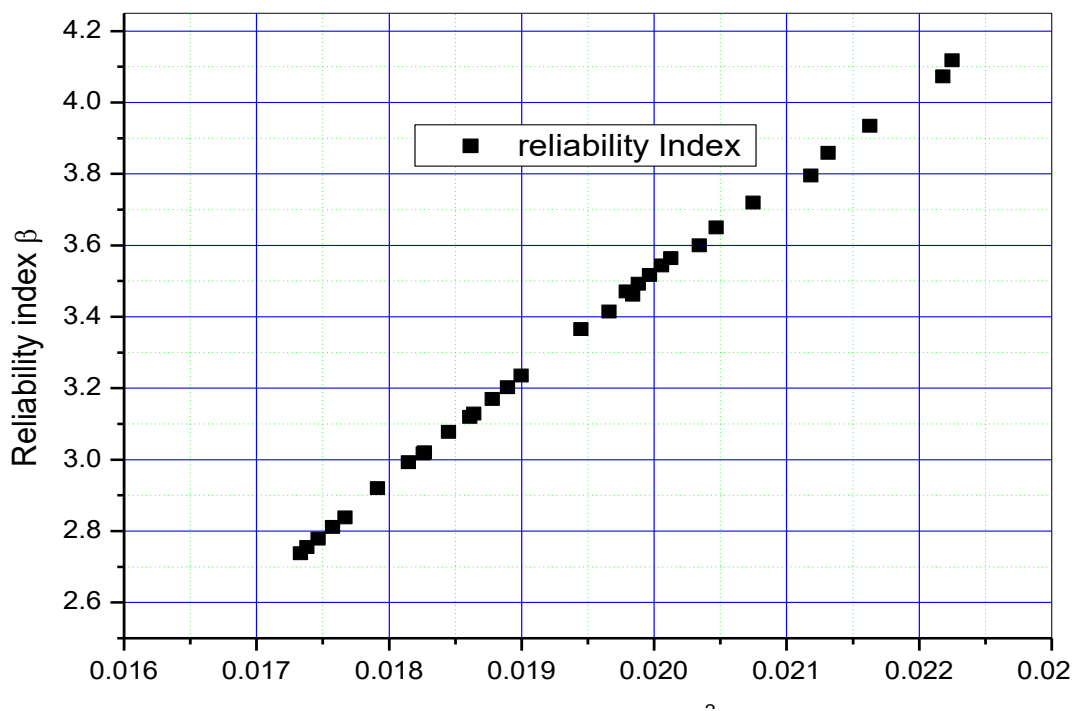
The final values of each Beta index and its corresponding objective function values are listed in Table 18. The reliability index β , as a function of the net sectional area, is shown in Figure 4.7. The minimum and maximum values of the Beta index of all design solutions at the Pareto frontier are 2.737 and 4.11.

The design solution n° 6, $\beta = 3.72$ fits all constrains of the two objective functions and the required safety target level, as defined to be here, $\beta_{target} = 3.7$.

Table 18 Beta index vs. corresponding objective function values

Net sectional area(m ²)	Displacement (m)	D	Beta
0.017912258	-0.001685744	0.892491	2.920072
0.020745972	-0.000876444	0.574452	3.719806
0.02118337	-0.00086262	0.539597	3.795665
0.018147679	-0.001627286	0.858206	2.992645
0.019448739	-0.001519276	0.697237	3.365486
0.02225042	-0.000561273	0.465629	4.118175
0.017381151	-0.001711997	0.97683	2.755372
0.02012654	-0.00090829	0.62914	3.563476
0.018450188	-0.001474753	0.816681	3.077679
0.017669372	-0.001469257	0.929804	2.838276
0.018779335	-0.001460376	0.774487	3.169698
0.019882135	-0.000966396	0.652628	3.491833
0.019967124	-0.000947233	0.64433	3.516402
0.017332506	-0.001609651	0.985078	2.737298
0.018259104	-0.001647469	0.84259	3.017329
0.019790815	-0.001491975	0.661704	3.471237
0.017574524	-0.001734474	0.94494	2.811562
0.019661817	-0.001398015	0.674814	3.414071
0.020341371	-0.001382517	0.609416	3.600005
0.018894587	-0.001442585	0.760401	3.202583

0.017466846	-0.001736792	0.962524	2.778962
0.018998057	-0.00144575	0.748044	3.235567
0.020469015	-0.001474592	0.598086	3.650192
0.020057212	-0.000921904	0.635687	3.543823
0.022178172	-0.001064937	0.470195	4.072389
0.018267844	-0.001646128	0.841381	3.020032
0.019838179	-0.001371968	0.656976	3.461805
0.018639272	-0.001638337	0.792078	3.128359
0.021313278	-0.000753048	0.52979	3.858709
0.021628463	-0.001107928	0.506965	3.934746
0.018611065	-0.001643947	0.795685	3.119889



4.6 Summary

A 175,000-ton bulk carrier is selected as a target ship. The stiffened plate located at the bottom of this ship is specified as the optimisation design task. The basic geometry parameters and location of the stiffened plate is described firstly, and then the calculation of the loading on the stiffened plate is described in 4.2. Optimisation procedure and relevant objective functions and constraint were stated in 4.3. In 4.4, the distributions of the random variables were estimated, and reliability based optimisation was performed. The optimisation results were presented and analysed in 4.5. The optimisation result of the stiffened plate on the reliability index of 3.72 is set. The section area of the optimised stiffened plate reduced 7.78%.

Chapter 5 Conclusions and future works

5.1 Conclusions

The objective of this work was to perform a multi-objective nonlinear structural optimisation of a stiffened plate subjected to combined stochastic compressive loads accounting for the ultimate strength and reliability based constraints in the design. The solution of the three-objective structural response, in minimising the weight, structural displacement and fatigue damage, was considered. The Pareto frontier solution was used to define the feasible solution of the design variables.

The reliability index, which defines the shortest distance from the origin to the limit-state boundary, was employed to identify the topology of the stiffened plate as a part of the Pareto frontier solution.

Comparing with the original section area, the optimised section area was reduced by 7.78%.

The presented methodology is flexible and demonstrated an excellent capacity to be used in the structural design of complex systems.

5.2 Future works

For improving the precision of optimisation results, the load calculation based on the first principle or numerical simulation should be performed. The sensitivities of the design and random variables should be analysed to demonstrate the most influencing ones and to derive the partial safety factors which can be used in the conception design, avoiding a complex structural analysis, which is one of the objectives of the project.

References

- [1] Vedeler G. To what extent do brittle fracture and fatigue interest shipbuilders today. Houdremont Lecture 1962, Sveiseteknikk, 192.(3)
- [2] Jordan C R, Cochran C S. In-service performance of structural details. SSC – 272, 1978
- [3] Jordan C R, Cochran C S. Further survey of in-service performance of structural details. SSC – 294, 1980
- [4] Munse W H. Fatigue criteria for ship structure details. Presented at the SNAME meeting on Extreme Loads Response Symposium, Arlington, VA, Oct. 19 – 20, 1981. 231 – 247
- [5] Munse W H. Fatigue characterisation of fabricated ship details for design. SSC – 318, 1983
- [6] Chen Y K, Chiou J W, Thayamballi A K. Validation of fatigue life prediction using containership hatch – corner strain measurements. SNAME Transactions, 1986, 94: 255 – 282
- [7] Clarke J D. Prediction of fatigue cracking in warship hulls. PRADS'87, Trondheim, Norway, June 1987:718 -728
- [8] Clarke J D. Fatigue crack initiation and propagation in warship hulls. In Smith C S and Dow R S(eds), Advances in Marine Structures, Elsevier Science Publishers Ltd, 1991. 42 – 60
- [9] Wirsching P H, Chen Y N. Considerations of probability-based fatigue design for marine structures. Marine Structures, 1988, 1:23–45
- [10] Xue J, Pittaluga A, Cervetto D. Fatigue damage calculation for oil tanker and container ship structures. Marine Structures, 1994, 7: 499 – 535
- [11] Hansen P F, Winterstein S R. Fatigue damage in the side shells of ships. Marine Structures, 1995,8: 631 – 655
- [12] Fricke W, Scharrer M, Selle H V. Integrated fatigue analysis of tanker structures. The 6th International Symposium on Practical Design of Ships and Mobile Units (PRADS'95), Seoul, Sept, 17 – 22, 1995, 2: 910 – 921
- [13] Proceedings of the 11th International Ship and Offshore Structures Congress (ISSC'91). WUXI, China, 1991
- [14] Proceedings of the 12th International Ship and Offshore Structures Congress (ISSC'94). St. John's, Canada, 1994
- [15] Proceedings of the 13th International Ship and Offshore Structures Congress (ISSC'99). Trondheim, Norway, August 18 – 23, 1997
- [16] Committee on Marine Structures. Prevention of Fracture in Ship Structure. Washington, D. C., 1997
- [17] GL. Rules for Classification and Construction. I – Ship Technology, Part 1 – Seagoing Ship. Chapter 1 – Hull Structures, Section 20 Fatigue Strength, Germanischer Lloyd, 1997
- [18] DNV. Fatigue Assessment of Ship Structures. Tech. Rep. DNVC 93 – 0432, Det Norske Veritas, 1995
- [19] ABS. Rules for Building and Classing Steel Vessels. Pt. 5, Sect. 2, A2AA. Guide for Fatigue Strength Assessment of Tankers and Bulk Carriers, American Bureau of Shipping, 1966
- [20] BV. Fatigue Strength of Welded Ship Structures. NI393 DSMROOM, Bureau Veritas, 1994
- [21] KR. Guidance for the Fatigue Strength Assessment of Ship Structures. Korean Register of Shipping, 1995
- [22] LR. ShipRight FDA, Fatigue Design Assessment Procedure, Structural Detail Design Guide.

Lloyd's Register of Shipping, 1996

[23] NK. Guidance for Fatigue Design of Ship Structures. Class NK, Nippon Kaiji Kyokai, 1996

[24] RINS. Rules for the Checking of the Fatigue Strength of Ship Hull Structures. Genova, Italy, 1995

[25] Han Qiang, Zhang Sanyuan, Yang Guitong, Advance in research for static and dynamic of buckling of structures, Advance in Mechanics, 1998, Vol.28(3):349-360

[26] He Fuzhi, Wang Zhengquan, A simplified progressive collapse analysis of ultimate longitudinal strength of ship structures, Journal of Ship Mechanics, 2001, Vol.5(5):21-35(in Chinese)

[27] Bai Yong, Xu Xiangdong, Cui Weicheng, Influence parameters and sensitivity for ultimate strength of ship structures, Journal of Ship Mechanics, 1998, Vol.2(5): 35-43(in Chinese)

[28] Xu Xiangdong, Cui Weicheng, Buckling and ultimate strength analysis of stiffened panels, Shipbuilding of China, 1999, No.144: 35-43(in Chinese)

[29] Busino G, Pareto V. L'Italia di Vilfredo Pareto: Economia e societa in un cteggio del 1873-1923. Banca Commerciale Italiana, 1989.

[30] Schaffer J D. Multiple Objective Optimization with Vector Evaluated Genetic Algorithms[C]//Proceedings of the 1st International Conference on Genetic Algorithms. L. Erlbaum Associates Inc. 1985: 93 – 100.

[31] Goldberg D E, Richardson J. Genetic algorithms with sharing for multimodal function optimisation, International Conference on Genetic Algorithms and Their Application. L. Erlbaum Associates Inc. 1987: 41 – 49

[32] Fleming P J. Genetic Algorithm for Multi-objective Optimization: Formulation, and Generalization[C]//International Conference on Genetic Algorithms. 1993.

[33] Srinivas N, Deb K. Deb, K.: Multiobjective Optimization Using Nondominated Sorting in Genetic Algorithms. Evolutionary Computation 2(3), 221-248. Evolutionary Computation, 1994, 2(3): 221-248

[34] Horn J, Nafpliotis N, Goldberg D E. A niched Pareto genetic algorithm for multiobjective optimisation Evolutionary Computation, 1994. IEEE World Congress on Computational Intelligence. Proceedings of the First IEEE Conference on IEEE, 1994, vol.1:82-87

[35] Garbatov Y. & Georgiev P., Optimal design of stiffened plate subjected to combined stochastic loads, Progress in the Analysis and Design of Marine Structures – Guedes Soares & Garbatov (Eds), 2017, Taylor & Francis Group, London, ISBN 978-1-138-06907-7:243-252

[36] Garbatov Y. & Dong Y., Fatigue reliability of butt-welded joints based on spectral fatigue damage assessment, Maritime Transportation and Harvesting of Sea Resources – Guedes Soares & Teixeira (Eds), 2018 Taylor & Francis Group, London, 611-616

[37] DNV. "Fatigue Assessment of Ship Structures". In: Classification Notes 30.7 Hovik: Det Norske Veritas, 2014.

[38] Garbatov, Y., Tekgoz, M. & Guedes Soares, C. 2011. Uncertainty assessment of the ultimate strength of a stiffened panel. In: Guedes Soares, C. & Fricke, W.(eds.) Advances in Marine Structures. London, UK: Taylor & Francis Group, 659–668.

[39] IACS, Common Structural Rules for Bulk Carriers and Oil Tankers, 2017

[40] Garbatov, Y. & Guedes Soares, C. 2008. Reliability of aged ship structures. In: Paik, J. & Melchers, R. (eds.) Condition Assessment of Aged Structures. Cambridge, UK: Woodhead Publishing Limited, 253–286.

- [41] Garbatov, Y. & Guedes Soares, C. 2011. Fatigue reliability assessment of welded joints of very fast ferry subjected to combined load. *International Journal of Maritime Engineering (RINA Transactions Part A)*, 153, 231–241.
- [42] Hasofer A M, Lind N C. Exact and invariant second-moment code format. *Journal of the Engineering Mechanics Division*, 1974, 100(1): 111-121.
- [43] Rackwitz R U D, Flessler B. Structural reliability under combined random load sequences. *Computers & Structures*, 1978, 9(5): 489-494.
- [44] Paloheimo E, Hannus M. Structural design based on weighted fractiles. *Journal of the Structural Division*, 1974, 100(7): 1367-1378.
- [45] DNV 2014. Structural Reliability Analysis of Marine Structures. Classification notes No 30.6. Hovik: DnV.
- [46] Guedes Soares, C., Dogliani, M., Ostergaard, C., Parmentier, G. & Pedersen, P.T. 1996. Reliability-Based Ship Structural Design. *Transactions of the Society of Naval Architects and Marine Engineers (SNAME)*, 104, 359–389.
- [47] Guedes Soares, C. & Moan, T. 1988. Statistical Analysis of Still-Water Load. Effects in Ship Structures. *SNAME Transactions*, 96, 129–156.
- [48] Guedes Soares, C. 1990. Stochastic Modelling of Maximum Still-Water Load Effects in Ship Structures. *Journal of Ship Research*, 34, 199–205.
- [49] Komuro, R., Ford, E.D. & Reynolds, J. 2006. The use of multi-criteria assessment in developing a process model. *Ecological Modelling*, 197, 320–330.
- [50] Timoshenko, S. P. and Gere, J. M., 1986, *Theory of Elastic Stability*: McGraw-Hill Book Company.
- [51] MARS2000, 2011, Bureau Veritas, Rules for the Classification of Ships and IACS Common Structural Rules for Bulk Carriers and Tankers: Bureau Veritas.-
- [52] Shimansky, 1956, *Shipbuilding mechanics*, Leningrad: Sudprogiz.
- [53] Guedes Soares, C., Dogliani, M., Ostergaard, C., Parmentier, G. and Pedersen, P. T., 1996, "Reliability-Based Ship Structural Design", *Transactions of the Society of Naval Architects and Marine Engineers (SNAME)*, 104, 359-389.
- [54] Guedes Soares, C. and Moan, T., 1988, "Statistical Analysis of Still-Water Load. Effects in Ship Structures", *Transactions of the Society of Naval Architects and Marine Engineers (SNAME)*, 96, 129-156.